Impact of CYP2C8 single nucleotide polymorphisms on in-vitro metabolism of imatinib to N-desmethyl imatinib

Muhammad Suleman Khan

Discipline of Pharmacology

School of Medical Sciences, Faculty of Health Sciences,

University of Adelaide

March, 2015

A thesis submitted for the degree of Master of Philosophy (Pharmacology)

Table of Contents

Abstract

Imatinib is a first line therapy for the treatment of chronic myeloid leukaemia (CML). Treatment with imatinib must be continuous and indefinite for most patients to maintain disease control. Despite excellent efficacy and tolerability, up to 50% of CML patients discontinue imatinib due to lack of efficacy and adverse events. Imatinib is metabolised to its main metabolite N-desmethyl imatinib by CYP3A4 and CYP2C8. *In vitro* human liver microsome (HLM) studies indicate imatinib autoinhibition of CYP3A4-mediated metabolism, suggesting a more significant role for CYP2C8 upon chronic dosing.

CYP2C8 is polymorphic and functional effects of the major *CYP2C8* polymorphisms *CYP2C8*3* and *CYP2C8*4* on N-desmethyl imatinib formation are unknown. It was hypothesised that *CYP2C8*3* and *CYP2C8*4* genetic polymorphisms will decrease imatinib metabolism to N-desmethyl imatinib in HLM. Therefore the aim of this study was to examine the impact of *CYP2C8*3* and *CYP2C8*4* on N-demethylation of imatinib in HLMs genotyped for *CYP2C8*1/*1* (n=5), *CYP2C8*1/*3* (n=4), *CYP2C8*1/*4* (n=2), in *CYP2C8*3/*3* pooled HLM, and in expressed CYP2C8 and CYP3A4 enzymes. Effects of CYP-selective chemical and antibody inhibitors on N-demethylation were also determined.

A single enzyme Michaelis-Menten model with substrate inhibition best fitted wild-type *CYP2C8*1/*1* HLM kinetic data (median ± SD K_i = 139 ± 61 µM). Three of four *CYP2C8*1/*3* HLMs showed single enzyme but no substrate inhibition kinetics. Binding affinity (K_m) was approximately 2-fold higher in *CYP2C8*1/*3* HLMs as compared to *CYP2C8*1/*1* (median ± SD K_m = 6 ± 2 *vs* 11 ± 2 µM, p=0.04). Intrinsic clearance (Cl_{int}) was higher in *CYP2C8*1/*3* HLMs compared to *CYP2C8*1/*1* (median ± SD Cl_{int} = 19 ± 8 *vs* 13 ± 2 µl/min/mg, p = 0.25).

*CYP2C8*3/*3* (pooled HLM) showed highest binding affinity (K_m = 3.6 µM) and weak autoinhibition (K_i = 449 µM) kinetics. N-desmethyl imatinib formation was below the limit of quantification in one *CYP2C8*1/*4* HLM, whereas the other *CYP2C8*1/*4* HLM showed lower intrinsic clearance (Cl_{int} = 7 *vs* 11 ± 2 µl/min/mg) due to 2-fold lower catalytic activity (V_{max}) compared to the wild-type (V_{max} = 73 *vs* 140 ± 31 pmol/min/mg).

A single enzyme model with substrate inhibition best fitted expressed CYP2C8 kinetic data (K_i = 149 µM). Expressed CYP3A4 showed two site enzyme kinetics with no evidence of autoinhibition. CYP2C8 inhibitors reduced N-demethylation in HLM by 47-75%, compared to 0-30% for CYP3A4 inhibitors. Two unidentified peaks M1 and M2 were found in expressed CYP3A4, whereas they were absent in expressed CYP2C8. These results indicate that *CYP2C8*3* may enhance CYP2C8 activity by influencing autoinhibition, and that *in vitro* the metabolism and autoinhibition of imatinib N-demethylation appears mainly mediated by CYP2C8 and not CYP3A4. *CYP2C8*4* appears a reduced functional allele for imatinib N-demethylation.

Declaration

This work contains no material which has been accepted for the award of any other degree or diploma in any University or other tertiary institution and, to the best of my knowledge and belief, contains no materials previously published or written by another person, except where due reference is made in the text.

I give consent to this copy of my thesis, when deposited in the University Library, being available for loan and photocopying, unless permission has been granted by the University to restrict access for a period of time.

Adelaide, March 2015

Muhammad Suleman Khan

Acknowledgements

I would like to express my sincere thanks to my principal supervisor Professor Andrew Somogyi for giving me opportunity to conduct this research, for your support and guidance during the study.

My sincere thanks to my co-supervisor Dr. Daniel Barratt, for your continuous guidance and support from laboratory work to the writing of this thesis.

The research presented in this thesis would not have been possible without funding from the University of Adelaide International Post Graduate Research Scholarship, as well as financial assistance from Faculty of Health Sciences, University of Adelaide.

To my family, thank you for your prayers and support.

To my wife, thank you for your love and care.

List of Abbreviations

ABL	Abelson murine leukaemia oncogene
AUC	Area under the plasma concentration-time curve
BCR	Break point cluster region gene
^{o}C	Degree Celsius
CI	Confidence interval
Cl_{int}	Intrinsic clearance
C_{max}	Maximum plasma concentration
CML	Chronic myeloid leukaemia
C_{trough}	Trough plasma concentration
CV	Co-efficient of variation
CYP450	Cytochrome P450
Cyt b5	Cytochrome b5
DL	Symbol for racemic mixture
DNA	Deoxyribonucleic acid
ER	Endoplasmic reticulum
h	Hill slope
HLM	Human liver microsomes
HLS	Human liver sample
HPLC	High performance liquid chromatography
HSA	Human serum albumin
IC_{50}	Half maximal inhibitory concentration
K_i	Substrate inhibition constant
K_m	Michaelis-Menten constant
LC-MS	Liquid chromatography mass spectrometry
LOQ	Limit of quantification
MAB-3A	Monoclonal antibody inhibitor of human CYP3A4

MAB-2C8	Monoclonal antibody inhibitor of human CYP2C8
µg	Microgram(s)
µl	Microliter(s)
µM	Micromolar
mg	Milligrams(s)
min	Minutes
ml	Milliliter(s)
mM	Millimolar
ng	Nanogram(s)
NADPH	Nicotinamide adenine dinucleotide phosphate
NDIM	N-desmethyl imatinib
p	Probability
Ph^+	Philadelphia chromosome
pmol	Picomole
QC	Quality control
rs	Reference SNP ID number
S	Substrate concentration
S_9	Supernatant fraction from liver (centrifuging at 9000 x g)
SD	Standard deviation
SNP	Single nucleotide polymorphism
$t_{1/2}$	Plasma half life
TKI	Tyrosine kinase inhibitor
UV	Ultraviolet
UGT	Uridine glucuronyl transferase
v	Reaction rate
Vd	Volume of distribution
V_{max}	Maximum formation rate

Chapter 1: Introduction

1. Imatinib

Imatinib was the first successful molecularly-targeted chemotherapy among the novel class of drugs called tyrosine kinase inhibitors (TKIs), and is now used as a first line therapy in newly diagnosed chronic myeloid leukaemia (CML) patients. It is also used in Philadelphia chromosome positive (Ph^+) acute lymphoblastic leukaemia and *c-KIT* and *PDGFR* positive gastrointestinal stromal tumour (Linch et al. 2013;Jabbour and Kantarjian 2014;Maino et al. 2014). Each year in Australia 330 people are newly diagnosed with CML (leukaemia.org.au). Treatment failure results in mortality. Imatinib has revolutionised treatment in CML by improving the 10-year overall survival from 20% to 80-90% (Jabbour and Kantarjian 2014). In Australia three TKIs, imatinib, dasatinib and nilotinib, are recommended as a first line treatment in CML (leukaemia.org.au).

1.1 Mechanism of action of imatinib

CML is a cancer of white blood cells caused by a somatic genetic abnormality called the Philadelphia chromosome (Ph^+) in myeloid cells of the bone marrow. Ph^+ is formed as a result of a balanced reciprocal translocation between the abelson murine leukemia (*ABL*) gene on chromosome 9 and the break point cluster region gene (*BCR*) on chromosome 22 resulting in the formation of a *BCR-ABL* gene. The product of *BCR-ABL* is a constitutively active tyrosine kinase onco-protein (BCR-ABL) which is the basis of CML pathogenesis (Daley et al. 1990). BCR-ABL phosphorylation activity results in a cascade of signalling pathways which cause pathological cell proliferation and survival (Goldman and Melo 2003). Imatinib binds to the ATP

binding site of BCR-ABL, inhibiting its phosphorylation activity and hence proliferations of the cancer clone (Druker et al. 2001). Treatment with imatinib is generally well tolerated, but currently must be continuous and indefinite for most patients to maintain disease control. In cases of sub-optimal responses to imatinib therapy, higher doses of imatinib, or substituting imatinib with second generation tyrosine kinase inhibitors, is recommended (Baccarani et al. 2009).

1.2 Efficacy of imatinib

The IRIS [International Randomized Study of Interferon and STI571 (imatinib)] study was a landmark clinical trial comparing the efficacy and safety of imatinib versus interferon alpha plus cytarabine (previously used standard treatment) in CML patients. Five hundred and fifty three patients were randomly assigned to receive imatinib 400 mg once daily or to receive interferon alpha plus cytarabine. After 5 years of follow up of patients still in treatment, overall survival rate and progression free survival was 89% and 97% in the imatinib arm, respectively (Druker et al. 2006). Eight years follow up of this study in patients who remained on imatinib treatment reported progression free survival and overall survival of 81% and 93%, respectively, and 45% of patients had discontinued treatment due to adverse events (6%), unsatisfactory therapeutic outcome (16%), stem cell transplantation (3%), death (3%) or other reasons (17%) (Deininger et al. 2009). Similar results were found recently in 1503 CML patients, of whom 1379 patients received imatinib alone. At 10 years, progression free survival and overall survival was 82% and 84%, respectively (Kalmanti et al. 2015). Recent evaluation of these patients showed that 36% of patients had discontinued imatinib due to inadequate response and adverse events (Kalmanti et al. 2015).

Data from clinical practice in 627 CML patients who had received imatinib also showed that 15% of patients present resistance to imatinib (as defined by the physician) and 31% experienced adverse events that led to discontinuation of imatinib (Michallet et al. 2010).

1.3 Clinical response assessment

Current guidelines identify multiple important milestones for optimal imatinib treatment, as well as definitions of suboptimal response and treatment failure, that predict long term outcomes (Jabbour and Kantarjian 2014). A failure to achieve a milestone response is generally categorised as either primary resistance (no response to the treatment) or secondary resistance (loss of initial treatment response) (Jabbour et al. 2013).

Recent study in 274 CML patients treated with imatinib 400 mg/day has shown that long-term response to TKIs can be predicted by measuring *BCR-ABL* transcript levels in blood as early as 3 months. Overall survival at 8 years, was significantly higher in patients with low (less than 9.8%) *BCR-ABL* transcript levels at 3 months as compared to the patients with higher transcript levels (93.5% *v* 55.6%, $P < 0.001$) (Neelakantan et al. 2013). Similarly another study in 282 CML patients on imatinib 400 mg/day found that the patients who had *BCR-ABL* transcripts less than 10% at 3 months had significantly better 8 year overall survival as compared to the rest of the patients (93.3% *v* 56.9%, $P < 0.001$) (Marin et al. 2012). These studies suggest that early molecular response is important to imatinib therapy in order to achieve the long term clinical benefits. However, approximately 25% of patients fail to achieve early molecular response due to primary resistance (Hanfstein et al. 2012;Marin et al. 2012;Neelakantan et al. 2013).

1.4 Mechanism of resistance to imatinib

The major known determinants of imatinib resistance are inadequate target site (intracellular) concentrations (primary and secondary resistance) and mutations in *BCR-ABL* (secondary resistance) (Jabbour et al. 2013). As shown in Figure 1.1, the former is determined firstly by unbound plasma concentrations (a product of dose, patient compliance, metabolism, and transport proteins), and secondly by transport proteins mediating imatinib uptake into the CML cells (Marin et al. 2010;Jabbour et al. 2013;Berglund et al. 2014;Widmer et al. 2014).

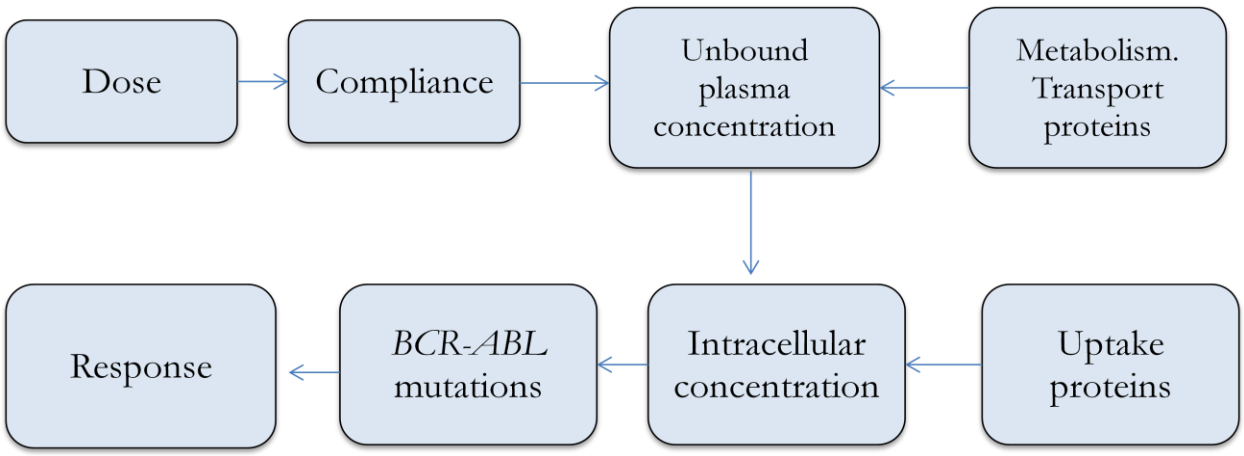

Figure 1.1: Mechanisms of primary and secondary resistance to imatinib treatment.

A correlation between trough plasma imatinib concentrations and clinical response to imatinib has been established by several studies. Total (bound+unbound) trough plasma imatinib concentrations of more than 1000 ng/ml are associated with significantly better clinical response, whereas plasma concentration below 1000 ng/ml is associated with poor clinical response in CML patients (Picard et al. 2007;Larson et al. 2008). On the other hand, adverse events such as

fluid retention, rash, anaemia, myalgia were more frequently reported in patients with trough plasma imatinib concentrations greater than 1165 ng/ml (Guilhot et al. 2012)

1.5 Variations in trough plasma imatinib concentrations

Trough plasma imatinib concentrations between patients administered the same dose of imatinib are highly variable, as shown by multiple studies (Table 1.1). Also, a significant number (~73%) of patients failed to achieve target trough plasma imatinib concentrations of 1100 ng/ml (Lankheet et al. 2014). It is important to identify factors which are contributing to these variations in order to minimise primary resistance.

Table 1.1: Interindividual variability in trough total plasma imatinib concentrations in CML patients.

Number of Patients	Dose	Parameter	Reference
68	400 mg (n=50) 600 mg (n=18)	Overall C_{trough} range: 181-2947 ng/ml $Mean_{400\ mg}$ ± SD: 1058 ± 557 ng/ml $Mean_{600\ mg}$ ± SD: 1440 ± 710 ng/mL	(Picard et al. 2007)
351	400 mg	C_{trough}: 153-3910 ng/ml Mean ± SD, CV %: 979 ± 530 ng/ml, 54%	(Larson et al. 2008)
87	400 mg	C_{trough} range: 203-4980 ng/ml Mean ± SD: 1378 ± 725 ng/ml	(Sohn et al. 2011)
190	400 mg	C_{trough} range: 25–3000 ng/ml	(Takahashi et al. 2010)
1216	400 mg – 800 mg	Dose-adjusted CV% = 60%	(Bouchet et al. 2013)

$C_{trough:}$ Trough total plasma imatinib concentration, SD: Standard deviation, CV: Co-efficient of variation.

1.6 Pharmacokinetic profile of imatinib

Imatinib is an orally administered drug and 400 mg per day is recommended as an initial dose in CML. It has a favourable pharmacokinetic profile. It is almost completely and rapidly absorbed from the gastrointestinal tract. Peak plasma concentrations (C_{max}) are reached after 2 hours of administration and mean bioavailability in healthy volunteers after a single oral dose of imatinib 400 mg was greater than 97% (Peng et al. 2004). However, interindividual variation was large in this study; co-efficient of variation (CV) was 44% for maximum plasma concentration (C_{max}), and 31% for area under the plasma concentration-time curve (AUC).

Food has no significant effect on the bioavailability of the imatinib (Peng et al. 2005). Imatinib has a large volume of distribution (median Vd = 435 L after an intravenous infusion of 100 mg over one hour) and a plasma half life ($t_{1/2}$) of 18-22 hours (Peng et al. 2004). Imatinib is approximately 95% bound to plasma proteins, mainly α1-acid glycoprotein (Kretz et al. 2004). After oral administration of radiolabelled imatinib approximately 65% of the systemic exposure corresponds to imatinib and 10% to its main metabolite N-desmethyl imatinib (Gschwind et al. 2005). Approximately 80% of the dose is excreted within a week mainly in the faeces (67% of the excreted dose) and also in urine (13%). Imatinib and N-desmethyl imatinib account for 28% and 13% of the dose in excreta, respectively (Gschwind et al. 2005).

1.7 Summary

Despite favourable pharmacokinetics and excellent efficacy of imatinib, approximately 50% of patients discontinue imatinib treatment. Trough plasma imatinib concentrations are correlated with efficacy and adverse events. Inter-individual variations in trough plasma imatinib concentrations are large (24-64%) (Bouchet et al. 2013;de Wit et al. 2015). Imatinib is a low

hepatic extraction drug as its predicted intrinsic hepatic clearance (14.8 L/hr) (Filppula 2014) is lower than hepatic blood flow (~90 L/hr); hence variability in steady-state total plasma imatinib concentration is a function of imatinib metabolism and plasma protein binding. Therefore, variable imatinib metabolism may be an important factor determining variable imatinib response.

2. Imatinib metabolism

2.1 Human CYP enzymes

In humans to date 57 functional CYP genes have been identified that are grouped into 18 groups and 43 subgroups on the basis of amino acid sequence homology. Members of families and subfamilies are 40% and 55% identical in amino acid sequence, respectively (Nelson 2006). CYP1, 2 and 3 are the most important families which metabolise approximately 80% of the clinically used drugs (Wilkinson 2005;Zanger and Schwab 2013). In addition to drug metabolism, CYP enzymes play important physiological roles such as metabolism of fatty acids, hormones, bile acids, eicosanoids, steroids, and vitamins (Nebert and Russell 2002). CYP enzymes are mainly expressed in the liver and intestine (Pelkonen et al. 2008).

CYP enzymes are haem-proteins having unique spectral properties (Guengerich 2008). They are called P450 enzymes because carbon monoxide combines with reduced forms of iron to form a pink CO-CYP complex that exhibits a UV absorption peak near 450 nm (Garfinkel 1958;Klingenberg 1958). A generally accepted mechanism of P450 drug oxidation cycle is shown in Figure 1.2. However, the steps may not proceed linearly as described and the substrate may bind and release at different steps (Guengerich 2008). CYP3A4 is the most important CYP enzyme, playing major role in metabolism of approximately 30% of currently existing drugs,

whereas the importance of other enzymes such as CYP2C8 is continuously growing (Pelkonen et al. 2008;Lai et al. 2009;Zanger and Schwab 2013).

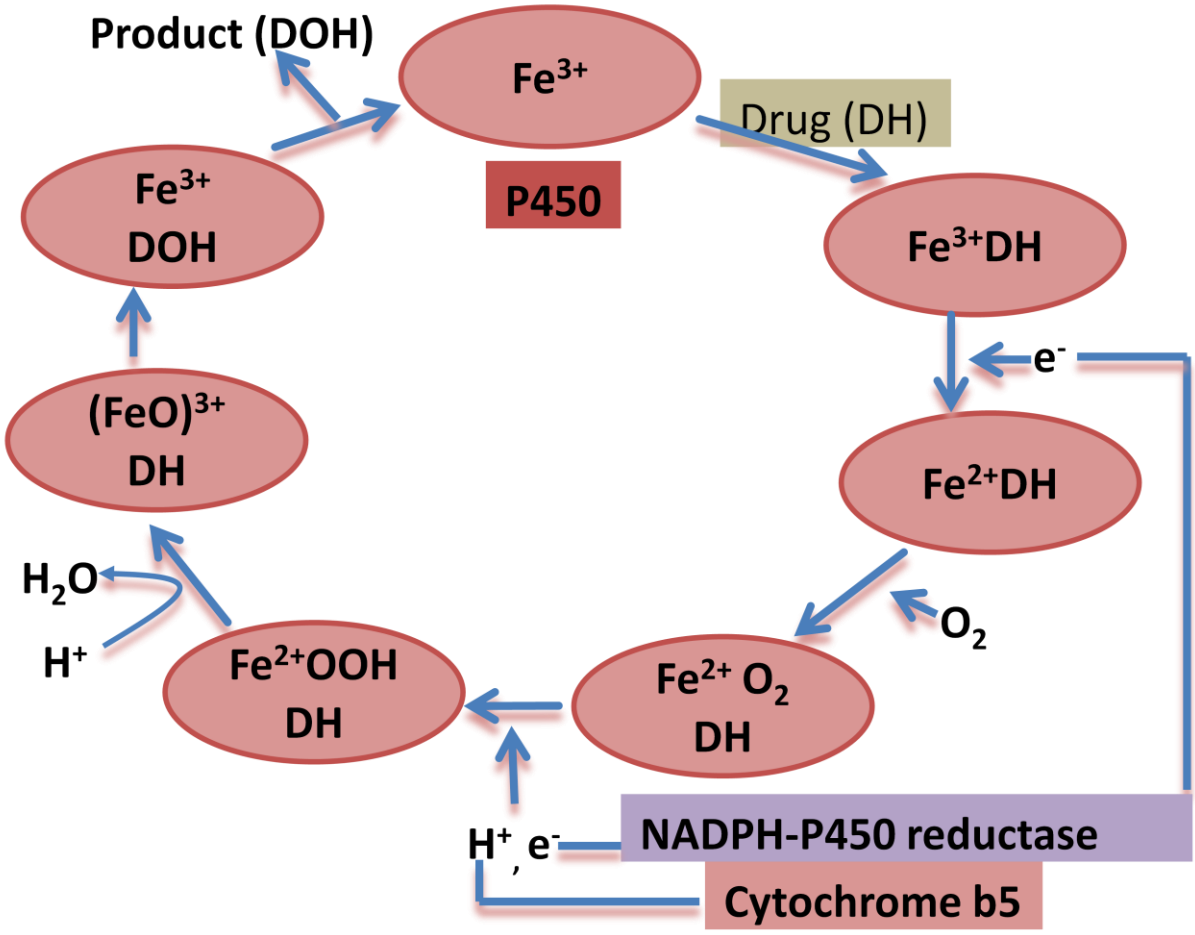

Figure 1.2: The P450 drug oxidation cycle. Ferric iron (Fe^{3+}) of CYP450 binds with substrate [drug(DH)]; Fe^{3+} reduces to Fe^{2+} by receiving an electron from NADPH-P450 reductase, which then combines with molecular oxygen, a proton and a second electron (either from NADPH-P450 reductase or from cytochrome b_5) to form an Fe^{2+}OOH-DH complex. This combines with another proton to yield water and a ferric oxene $(FeO)^{3+}$-DH complex. $(FeO)^{3+}$ extracts a hydrogen atom from DH, forms a pair of short-lived free radicals, liberates a product (DOH), and regenerates the P450 enzyme (modified and adapted from Rang et al. 1999).

2.2 Imatinib *in vitro* metabolism

Imatinib is metabolised to its main metabolite N-desmethyl imatinib (NDIM, CGP74588) by cytochrome P450 enzymes CYP3A4 and CYP2C8 (Nebot et al. 2010;Filppula et al. 2013a), with other CYP enzymes such as CYP1A1 and CYP1B1 (Rochat et al. 2008), CYP2C9, CYP2C19, CYP2D6 (Filppula et al. 2013a), CYP3A5 and CYP3A7 (Nebot et al. 2010) playing little or no role in imatinib metabolism. In addition to N-desmethyl imatinib, several other metabolites which include oxidative products and glucuronides have also been reported (Gschwind et al. 2005;Marull and Rochat 2006;Rochat et al. 2008;Filppula et al. 2013a). *In vitro*, CYP3A4 metabolises imatinib to N-desmethyl imatinib and other metabolites at a ratio of 1:3 (Figure 1.3); approximately 27% of the *in vitro* recombinant CYP3A4 metabolism (imatinib depletion) could be accounted for by NDIM formation (Filppula et al. 2013a). Imatinib CYP2C8 metabolism is primarily to N-desmethyl imatinib (Figure 1.3) (Filppula et al. 2013a). A previous study has reported that recombinant CYP3A5 catalyses imatinib N-demethylation with a similar affinity as CYP3A4 (44 and 43 μM respectively), however this study was limited by using few data points (Nebot et al. 2010). Recently, recombinant CYP3A5 was shown to have a minor effect on imatinib depletion; 80% of the parent drug was left after 30 minute incubation, with an estimated contribution of less than 1% to the total hepatic clearance via the N-demethylation pathway (Filppula et al. 2013a). Therefore the contribution of CYP3A5 was not investigated in this study.

2.2.1 Autoinhibition and mechanism-based inhibition

Autoinhibition is a type of inhibition where a compound is responsible for inhibition of its own metabolism. Autoinhibition can be reversible or irreversible. A previous study has reported autoinhibition of NDIM formation in recombinant CYP2C8 and CYP3A4 enzymes, with

estimated Ki values of 395 µM and 1400 µM, respectively (Filppula et al. 2012). Mechanism-based inhibition is an irreversible inhibition where a compound that is metabolised by an enzyme to an intermediate inactivates it before leaving the active site (Silverman, 1995). Specific experiments are required to classify a mechanism-based inhibition of an enzyme (Filppula et al. 2012).

Filppula et al (2012) investigated the *in vitro* time-dependent inhibitory effects of imatinib and N-desmethyl imatinib on CYP3A4 and CYP2C8 activity using midazolam 1'-hydroxylation and amodiaquine N-deethylation as marker reactions. The results of this study showed that imatinib is a potent mechanism-based inhibitor of CYP3A4 activity as the inhibitory effects was pre-incubation time, concentration, NADPH dependent and irreversible, whereas no time dependent inhibitory effects on CYP2C8 activity were found for either imatinib or N-desmethyl imatinib (Filppula et al. 2012). Assuming imatinib was a similar mechanism-based inhibitor of its own metabolism, *in silico* simulations based on these findings suggested, after multiple doses of imatinib 400 mg once daily, the fraction of drug metabolised by CYP2C8 would increase from 40% to 70%, and by CYP3A4 decrease from 60% to 30% (Filppula et al. 2013a), suggesting a more significant role for CYP2C8 enzyme in imatinib metabolism upon chronic dosing (Figure 1.3).

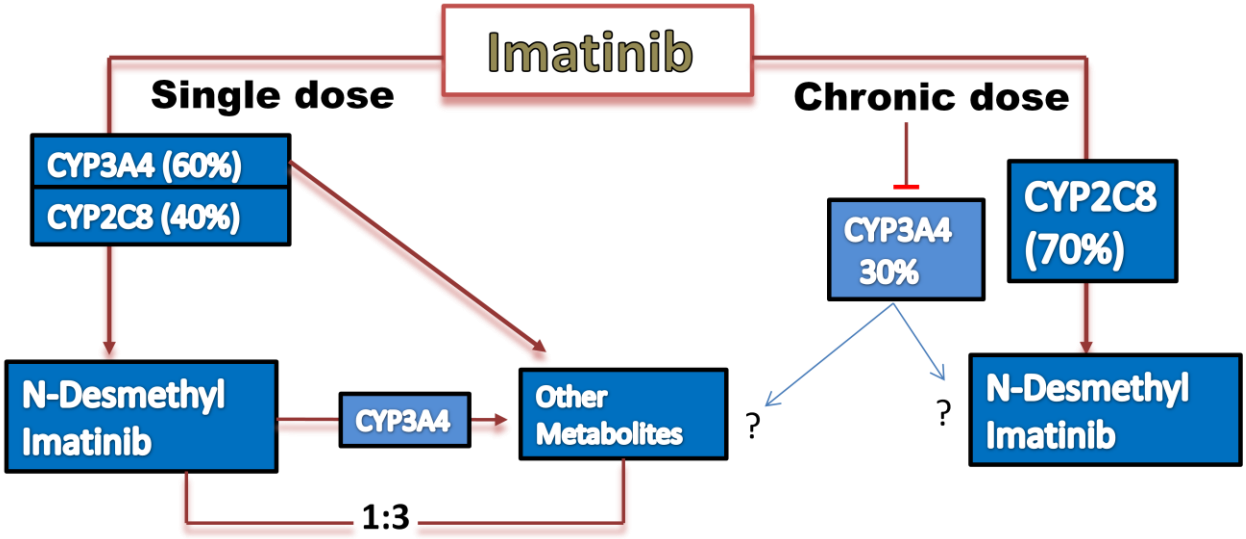

Figure 1.3: Important role for CYP2C8 in imatinib metabolism. Following a single oral dose, CYP3A4 and CYP2C8 are the main enzymes for imatinib metabolism to N-desmethyl imatinib (contribution of 60% and 40%, respectively). Upon chronic dosing, imatinib inhibits its own CYP3A4-mediated metabolism leading to increase in contribution of CYP2C8 (70%) to imatinib metabolism (Filppula et al. 2013a).

2.3 Imatinib *in vivo* interaction studies with CYP3A4 and CYP2C8 inhibitors/inducers

Co-administration of imatinib with CYP3A4 and CYP2C8 inhibitors and inducers can change the pharmacokinetics of imatinib. Fourteen healthy volunteers received an inducer of CYP3A4 (rifampicin 600 mg) for 10 days followed by a single dose of imatinib 400 mg. Imatinib C_{max} and AUC were decreased by 54% and 68%, respectively (Bolton et al. 2004). Rifampicin is also an inducer of other enyzmes and transporters such as CYP2C8 and ABCB1 (FDA. 2011), which might have contributed to these changes in pharmacokinetics. Following administration of the CYP3A4 inhibitor ketoconazole (400 mg), imatinib C_{max} and AUC_{0-24} increased by 26% ($P<0.005$) and 40% ($P<0.0005$), respectively, whereas AUC_{0-24} of N-desmethyl imatinib

decreased by only 13% ($P<0.05$) and no significant decrease in $AUC_{0-\infty}$ of NDIM was found ($P=0.28$) (Dutreix et al. 2004), suggesting metabolic pathways in CYP3A4 imatinib metabolism other than N-desmethyl imatinib formation, and CYP3A4 metabolism of N-desmethyl imatinib, are involved, as shown in Figure 1.3. In this study, other enzymes and transporters may also have contributed to changes in pharmacokinetics, as ketoconazole is also a moderate inhibitor of CYP2C8 (Lai et al. 2009) and ABCB1 (FDA. 2011). A previous study in 351 CML patients has shown no effect on steady-state imatinib clearance when administered with CYP3A4 inhibitors such as amiodarone, azithromycin, cimetidine, and inducers such as carbamazepine and rofecoxib (Schmidli et al. 2005). A confounding factor in this study was that the inhibitors tested are also inhibitors of other enzymes. For example, amiodarone is a weak CYP2D6 inhibitor, and cimetidine is a weak inhibitor of CYP2C19, however *in vitro* no significant contribution in imatinib metabolism was found for these enzymes (Filppula et al. 2013a). Recently, in a large observational study in 2478 CML patients, trough plasma imatinib concentrations at steady state were significantly lower in patients receiving any CYP3A4 inducers, such as carbamazepine and dexamethasone (630 *vs* 838 ng/ml, $P = 2 \times 10^{-6}$), and any P-gp inhibitors, such as ciclosporin and atorvastatin (682 *vs* 828 ng/ml, $P = 0.022$), and higher in patients receiving strong CYP3A4 inhibitors such as amiodarone and ritonavir etc. (983 *vs* 808 ng/ml, $P = 0.01$), compared to without such co-medications (Gotta et al. 2014).

To date only one study investigated the effect of a CYP2C8 inhibitor (gemfibrozil) on single dose imatinib (200 mg) pharmacokinetics. Gemfibrozil reduced the mean C_{max} and AUC of imatinib by 35 and 23%, respectively ($P < 0.001$). N-desmethyl imatinib C_{max} and AUC were reduced by 56% and 48% ($P < 0.001$) and the N-desmethyl imatinib/imatinib AUC ratio was reduced by 45% ($P < 0.001$). *In silico* simulation based on these results suggested inhibition of

an uptake transport protein explained reduced C_{max} and AUC, whilst inhibition of CYP2C8 might account for the change in metabolic ratio (Filppula et al. 2013b). A confounding factor in this study was that gemfibrozil is also inhibitor of other enzymes such as CYP1A2, CYP2C9, CYP2C19 (Wen et al.2001), however no significant contribution to imatinib metabolism was found for these enzymes *in vitro* (Filppula et al. 2013a).

2.5 Summary

In vitro CYP3A4 and CYP2C8 are the major enzymes in imatinib metabolism. The contribution of CYP3A4 to other metabolites is 3-fold higher than to N-desmethyl imatinib formation, whereas CYP2C8 metabolism is primarily to N-desmethyl imatinib. Imatinib is predicted to be a mechanism-based inhibitor of its own CYP3A4-mediated metabolism, leading to an important role for CYP2C8 enzyme in imatinib metabolism. Autoinhibition of NDIM formation in recombinant CYPs 2C8 and 3A4 is also reported. However, these studies had limitations (discussed in section 3.5) that warrant better characterisation of *in vitro* imatinib metabolism and any autoinhibition involved. In addition contribution of CYP3A4 and CYP2C8 using specific inhibitory antibodies has not been investigated previously. Furthermore, *CYP2C8* is polymorphic and its functional effects on imatinib metabolism have not been investigated yet.

3. *In vitro* drug metabolism

In vitro drug metabolism is an important tool to identify enzymes involved in the metabolism of a specific drug, potential drug interactions, and functional effects of genetic polymorphisms. Human enzyme sources which include human liver microsomes (HLM), liver slices or homogenates, hepatocytes, S_9 fraction and recombinant CYP enzymes are used to characterise *in*

vitro drug metabolism (Fasinu et al. 2012). Each test system has its own advantages and disadvantages. Liver slices or homogenates and hepatocytes contain all hepatic enzymes and drug transporters; however they are limited by availability and due to specific requirements such as viability testing, proper choice of media, support matrices, and careful preparation techniques (Fasinu et al. 2012;Ong et al. 2013). The other sources, HLM and expressed enzymes are the easiest way to study drug metabolism. However, they do not contain all the enzymes and lack drug transporters (see below).

To determine CYP involvement in drug metabolism, the following approaches are generally used:

- Correlating formation rate of the test drug metabolite with that of enzyme specific substrate using HLM
- Use of a selective chemical inhibitor or inhibitory antibody against a specific enzyme
- Using expressed enzyme

3.1 Human liver microsomes

CYP enzymes are mainly located in the liver. Within the liver cells they are mainly located in the smooth endoplasmic reticulum (ER). On homogenisation and differential centrifugation ER is broken to small fragments called microsomal fractions, commonly used to study the *in-vitro* drug metabolism (Rang et al. 1999). Microsomes as compared to hepatocytes are more readily available and CYP kinetic measurements are not confounded by other process such as cellular uptake. Microsomes are easy to use and can be stored for several years. However, they only contain phase I and UGT (Uridine glucuronyl transferase) enzymes (Pelkonen and Turpeinen 2007). Large variations are also found in microsomal preparations from different tissue sources.

In addition to being utilised in identifying a particular metabolic pathway and inhibition potency, microsomes are also utilised in studying inter-individual variations in drug metabolism (Ong et al. 2013).

3.2 Recombinant CYP enzymes

CYP proteins expressed in human lymphoblastoid cells, baculovirus insect cells, bacterial cells or yeast cells provide a reliable test system to study the contribution of an individual enzyme or variant in drug metabolism. They are also used to confirm results obtained from HLM studies. They are commercially available from several sources. However, only one enzyme can be studied at one time and variations in activity may arise when using different expression systems (Ong et al. 2013).

3.3 Enzyme kinetics

The most widely used kinetic parameter to determine *in vitro* enzyme activity is the intrinsic clearance (Cl_{int}) (Pelkonen and Turpeinen 2007) which is calculated as

$$CL_{int} = V_{max} / K_m \quad (1.1)$$

Where V_{max} is maximum formation rate and K_m is the Michaelis-Menten constant, equivalent to the substrate concentration [S] at which reaction rate is half its maximum.

The reaction is performed at 37°C in an incubation medium, consisting of microsomes or expressed enzymes, NADPH regenerating system and a buffer to maintain pH at 7.4. The rate of product formation is measured at multiple substrate concentrations. V_{max} and K_m is usually calculated by using Michaelis-Menten equation (Eq. 1.2) assuming the involvement of a single enzyme.

$$v = V_{max} * [S] / (K_m + [S]) \quad (1.2)$$

It is important to mention here for many drug metabolism reactions, simple Michaelis-Menten kinetics is not followed. In such cases enzyme kinetics may involve biphasic (two enzyme activities), substrate inhibition or sigmoidal (activation) kinetics. These atypical behaviours have a significant impact on the calculation of kinetic parameters; hence data should be analysed with caution using modified equations which represent such kinetic behaviours (Houston and Kenworthy 2000;Houston and Galetin 2005;Ong et al. 2013).

An important approach to identify atypical enzyme kinetics is to use Eadie-Hofstee plots, which are a diagnostic representation of enzyme kinetics in which reaction rate (V) is plotted as a function of the ratio between rate and substrate concentration (V/[S]). A linear Eadie-Hofstee plot is suggestive of involvement of one enzyme. A non-linear Eadie-Hofstee is suggestive of involvement of two or more enzymes or substrate binding sites. At higher concentrations some substrates also inhibit the enzyme activity. An Eadie-Hofstee plot displaying a downward curve in the upper left quadrant is suggestive of substrate inhibition (Miners et al. 2010). Substrate inhibition involving one enzyme can be described by the following equation.

$$v = V_{max} * [S] / (K_m + [S] * (1 + [S] / K_i)) \quad (1.3)$$

where K_i is the substrate inhibitor constant, equivalent to the substrate concentration [S] at which half of the V_{max} is inhibited.

3.4 Loss and gain of function in enzyme activity

In vitro the difference in enzyme activity between wild type and variant enzymes is measured by intrinsic clearance. Higher intrinsic clearance indicates gain of function which may be due to higher binding affinity (K_m) and/or higher catalytic activity (V_{max}), and lower intrinsic clearance indicates loss of function.

3.5 Limitations of previous *in vitro* imatinib metabolism studies

Previous kinetic studies of imatinib metabolism in HLMs and recombinant enzymes were limited by using too few data points. In one study, a non-linear Eadie-Hofstee plot for N-desmethyl imatinib formation in recombinant CYP3A4 was forced through a linear model (Rochat et al. 2008) and the result was based on a small number of data points (n = 5). Similarly in another study, Eadie-Hofstee plots were lacking and only 4 data points were used in recombinant CYP2C8 and CYP3A4 enzymes, which makes the calculation of kinetic parameters unreliable (Nebot et al. 2010). In another kinetic study of recombinant CYP3A4 enzyme, the estimated inhibition constant (K_i) value calculated was 4-fold greater than the maximum substrate concentration used (320 µM) (Filppula et al. 2013a). Since at least two enzymes are shown to participate in imatinib metabolism with evidence of autoinhibition (Filppula et al. 2013a), a sufficient number of data points are needed to clearly show any autoinhibition involved and to better characterise the kinetic parameters. In addition, the relative contributions of CYPs 3A4 and 2C8 to imatinib metabolism in HLM have not been investigated using specific monoclonal inhibitory antibodies. Furthermore, as mentioned above, *CYP2C8* is polymorphic and the effect of genetic variability in *CYP2C8* on imatinib metabolism to N-desmethyl imatinb has not been investigated as yet.

4. CYP2C8 and CYP3A4 enzymes

4.1 CYP2C8

The human CYP2C family consists of highly homologous genes located on chromosome 10q24 in the following order (centromere-CYP2C18-CYP2C19-CYP2C9-CYP2C8-telomere) (Totah and Rettie 2005). Approximately 25-30% of drugs are metabolised by the CYP2C family. CYP2C8 metabolises 5-7% of current drugs (Lai et al 2009). Our understanding of the importance of CYP2C8 is growing as many new substrates and inhibitors are identified (Table 1.2). CYP2C8 is the principal enzyme involved in the metabolism of some anticancer drugs (paclitaxel and debrafenib), antidiabetic drugs (pioglitazone, rosiglitazone and repaglinide), antimalarials (amodiaquine, chloroquine) and antibiotics such as trimethoprim (Table 1.2). Paclitaxel (preferable) and amodiaquine (acceptable) are model drugs for *in vitro* assessment of CYP2C8 activity, whereas montelukast and quercetin are preferable selective CYP2C8 inhibitors for *in vitro* activity (FDA. 2011).

CYP2C8 is the most inducible member of the CYP2C family (Lai et al. 2009). Rifampicin is a recommended *in vitro* inducer (FDA. 2011). Some drug metabolites such as gemfibrozil 1-O-ß-glucuronide, clopidogrel 1-O-ß-glucuronide are also inhibitors of CYP2C8 (Table 1.2).

CYP2C8 is mainly expressed in the liver and to a minor extent in the adrenal glands, kidney, brain, mammary glands and uterus (Totah and Rettie 2005). CYP2C8 also catalysed the oxidation of arachidonic acid to epoxyeicosatrienoic acid (EETs) that has important myocardial and respiratory functions (Delozier et al. 2007;Bajpai et al. 2014).

CYP2C8 has a larger active site (1438 $Å^3$) as compared to the other CYP enzymes (Schoch et al. 2008). It can accommodate large substrates and inhibitors such as paclitaxel and montelukast (Lai et al. 2009). The topology of the active site cavity is trifurcated resembling T or Y shape. In comparison CYP3A4 active site cavity is also large (1386 $Å^3$), however it is uniformly distributed that may explain why CYP2C8 and CYP3A4 often share common substrates but result in different metabolic products (Totah and Rettie 2005).

4.2 *CYP2C8* genetic polymorphism

CYP2C8 is a 31 kb gene consisting of 9 exons (Klose et al. 1999). *CYP2C8* is polymorphic and to date 16 CYP alleles have been identified (*CYP2C8*1A* to *CYP2C8*14*) (cypalleles.ki.se). *CYP2C8*5*, **7* and **11* are rare variants (<1%), resulting in a truncated protein and are associated with loss of function (cypallele.ki.se). *CYP2C8*5* to *CYP2C8*14* are also rare variants, found mainly in Asians with less than 1% frequency (Hichiya et al. 2005;Aquilante et al. 2013a). *CYP2C8*2*, *CYP2C8*3*, and *CYP2C8*4* are the most investigated variants with potential clinical consequences (Aquilante et al. 2013a).

*4.2.1 CYP2C8*2*

*CYP2C8*2* (rs11572103) is found only in Africans and African Americans with a frequency of 15-18%, is rare in Asians, and absent in Caucasians (Dai et al. 2001;Parikh et al. 2007;Aquilante et al. 2013b). *CYP2C8*2* has been associated with decreased *in vitro* enzyme activity and lower intrinsic clearance as compared to the wild type (Dai et al. 2001;Gao et al. 2010;Parikh et al. 2007).

Table 1.2: Examples of CYP2C8 substrates and inhibitors (modified and adapted from Lai et al. 2009 and Filppula. 2014).

Substrates	Class of Drug	Pathway	References
Amiodarone	Antiarrhythmic	N-deethylation	(Ohyama et al. 2000)
Amodiaquine	Antimalarial	N-deethylation	(Li et al. 2002)
Buprenorphine	Local anesthetic	N-dealkylation	(Picard et al. 2005)
Cerivastatin	HMG-CoA reductase inhibitor	hydroxylation & O-demethylation	(Wang et al. 2002)
Chloroquine	Antimalarial drug	N-deethylation	(Kim et al. 2003)
Debrafenib	Anti cancer	Oxidation	(Lawrence et al. 2014)
Fluvastatin	HMG-CoA reductase inhibitor	hydroxylation	(Wang et al. 2002)
Loperamide	Antidiarrheal drug/opioid	N-demethylation	(Kim et al. 2004)
Paclitaxel	Anti cancer	hydroxylation	(Rahman et al. 1994)
Pioglitazone	Antidiabetic drug	hydroxylation	(Jaakkola et al. 2006)
Repaglinide	Antidiabetic drug	hydroxylation	(Bidstrup et al. 2003)
R-ibuprofen	NSAID	hydroxylation	(Hamman et al. 1997)
Rosiglitazone	Antidiabetic drug	hydroxylation	(Baldwin et al. 1999)

Inhibitors	mechanism of inhibition	Reference
Clopidogrel acyl I-O-B-glucuronide	Mechanism-based inhibitor	(Tornio et al. 2014)
Gemfibrozil	Reversible (competitive)	(Ogilvie et al. 2006)
Gemfibrozil I-O-B-glucuronide	Mechanism-based inhibitor	(Ogilvie et al. 2006)
Ketoconazole	Reversible (non-competitive)	(Bun et al. 2003)
Montelukast	Reversible (competitive)	(Walsky et al. 2005)
Nilotinib	Reversible (competitive)	(Wang et al. 2014a)
Quercetin	Reversible (competitive)	(Bun et al. 2003)

HMG-CoA, 3-hydroxy-3-methyl-glutaryl-coenzyme A; NSAID, non-steroidal anti-inflammatory drug

4.2.2 *CYP2C8*3*

*CYP2C8*3* is a haplotype consisting of two non-synonymous single nucleotide polymorphisms (amino acid change; R139K, K399R) located in exon 3 (rs11572080) and exon 8 (rs10509681), respectively (Dai et al., 2001; Aquilante et al. 2013a). It is frequent in Caucasians (13-15%) (Dai

et al. 2001;Bahadur et al. 2002) and absent in Africans and Asians (Parikh et al. 2007; Aquilante et al. 2013a). The functional consequences of *CYP2C8*3* polymorphism are variable and appear substrate specific as discussed below.

4.2.2.1 Paclitaxel and Amodiaquine

For paclitaxel and arachidonic acid metabolites, the activity of *CYP2C8*3* variant expressed in E.coli was reduced by 85% and 40%, respectively, as compared to *CYP2C8*1* (Dai et al. 2001). Similarly in expressed *CYP2C8*3* variant in HepG2 (human hepatocellular carcinoma) cells, CL_{int} for paclitaxel 6α-hydroxylation was significantly lower compared to the wild type (1.88 ± 0.3 *vs* 1.35 ± 0.2, $P < 0.05$) (Soyama et al. 2001). For amodiaquine, reduced metabolism was found, with undetectable activity for the *CYP2C8*3* expressed variant (Parikh et al. 2007). Gao et al (2010) also characterised functional effects of *CYP2C8*3* variants expressed in yeast cells using paclitaxel 6α-hydroxylation and amodiaquine N-deethylation as a marker reaction. The CL_{int} for *CYP2C8*3* was 2-fold lower than the wild type, due to low binding affinity (K_m was 2-fold higher compared to the wild type, $P < 0.01$) (Gao et al. 2010).

Clinical studies have shown conflicting results for paclitaxel. In 93 ovarian cancer patients, clearance of unbound paclitaxel was reduced by 11% in patients with CYP2C8**1/*3* genotype as compared to the wild type, $P = 0.03$ (Bergmann et al. 2011). In another small study, paclitaxel clearance was 2-fold lower in 38 ovarian cancer patients with *CYP2C8*1/*3* as compared to the wild type, $P = 0.03$ (Green et al. 2009). Other studies have failed to replicate the lower activity associated with *CYP2C8*3* for paclitaxel metabolism (Taniguchi et al. 2005;Rowbotham et al. 2010). *CYP2C8*3* polymorphism was also found to be associated with an increased risk for

paclitaxel related neurotoxicity. *CYP2C8*1/*3* patients had significantly higher risk of motor neuropathy as compared to the wild type (P=0.034) (Green et al. 2009).

4.2.2.2 Anti diabetic agents

For antidiabetic drugs such as pioglitazone and repaglinide, higher activity was found (Muschler et al. 2009;Yu et al. 2013). For repaglinide, expressed *CYP2C8*3* variant showed 1.31-fold higher Cl_{int} than the *CYP2C8*1* enzyme ($P < 0.05$) (Yu et al. 2013). For pioglitazone metabolism to M-IV, CL_{int} was higher in **3/*3* HLMs (n=5) as compared to the wild type (n=5) (mean ± SD, 35 ± 9 *vs* 24 ± 4 pmol/min/mg/µM, P = 0.04) (Muschler et al. 2009). In this study **3/*3* HLMs were also carrying the *CYP2C9*2* polymorphism which is in partial linkage disequilibrium with *CYP2C8*3* (Yasar et al. 2002), that may have contributed to the overall activity. This study also found concentration-dependent autoinhibition of M-IV formation.

For antidiabetic agents the *in vivo* data appear to agree with the *in vitro* findings. For repaglinide at a dose of 0.25 mg, mean AUC and C_{max} were 45% and 39% lower in healthy subjects with *CYP2C8*1/*3* genotype as compared to the wild type ($P < 0.005$) (Niemi et al. 2003). Other studies have shown little or no effect of *CYP2C8*3* polymorphism on pharmacokinetics of repaglinide in healthy volunteers who received a more clinically relevant dose of 2 mg (Bidstrup et al. 2006;Tomalik-Scharte et al. 2011). The reason for this might be the difference in dose (2 vs 0.25 mg). For rosiglitazone, trough plasma concentrations in 187 type 2 diabetic patients were significantly lower in **1/*3* patients compared to the wild type (23.1 *vs* 16.5 ng/ml, P=0.03) (Stage et al. 2013). Similarly in healthy volunteers, single dose rosiglitazone AUC was decreased by 36% and 7% and clearance increased by 40% and 15% in **3/*3* and **1/*3* genotypes, respectively, as compared to the wild type, however the difference was only significant for **3/*3*

(P = 0.03), similar findings were also observed after multiple doses of rosiglitazone (Kirchheiner et al. 2006). For pioglitazone, in healthy subjects, AUC was decreased by 34% and 26% in **3/*3* and **1/*3*, respectively, compared to the wild type (P < 0.05) (Tornio et al. 2008). Data on other drug classes such as NSAIDs, opioids, statins and antimalarials are accumulating (Daily and Aquilante 2009), however they are complicated by the involvement of other enzymes such as CYP2C9 and CYP3A4.

4.2.3 *CYP2C8*4*

*CYP2C8*4* (rs1058930) is another important polymorphism that has functional consequences. It is found with an allele frequency of 7-8% in Caucasians, is absent in Asians, and rare in Africans (Bahadur et al. 2002; Aquilante et al. 2013a). For paclitaxel, lower activity was found for *CYP2C8*4* variants in HLMs, with median paclitaxel 6α-hydroxylation activity approximately 1.7-fold lower as compared to the wild type, however the difference was not statistically significant (P > 0.05) (Bahadur et al. 2002). *CYP2C8*4* expressed variants in E.coli showed only 15% of activity as compared to the wild type for paclitaxel 6α-hydroxylation (Singh et al. 2008). *CYP2C8*4* expressed variants in yeast cells also showed significantly lower activity for paclitaxel 6α-hydroxylation and amodiaquine N-deethylation (Gao et al. 2010). Paclitaxel CL_{int} was 3-fold lower in *CYP2C8*4* variant compared to wild type, due to low catalytic activity (P < 0.01). For amodiaquine N-deethylation, activity was approximately 1.5-fold lower compared to wild type only at low substrate concentration (P < 0.05) (Gao et al. 2010). The structure-functional relationship study showed that *CYP2C8*4* variant resulted in a reduced function protein with an inactive P420 state (Singh et al. 2008;Gao et al. 2010;Jiang et al. 2011). *In vivo* effects of *CYP2C8*4* on substrate pharmacokinetics are inconclusive, as too few subjects were included in clinical studies (Daily and Aquilante 2009). In some studies no significant effect of

*CYP2C8*4* genotype was found on paclitaxel and repaglinide pharmacokinetics (Niemi et al. 2003;Marsh et al. 2007).

4.2.4 Summary

These studies indicated that *CYP2C8*3* alters CYP2C8 enzyme activity both *in vitro* and *in vivo* in a substrate specific manner. For some substrates such as paclitaxel it leads to reduced *in vitro* activity, however *in vivo* data for paclitaxel is inconsistent. For anti-diabetic drugs, both *in vitro* and *in vivo* data indicated enhanced activity for *CYP2C8*3*, however data should be interpreted with care due to the contribution of other enzymes such as CYP2C9 and CYP3A4. No mechanism for loss or gain of function associated with *CYP2C8*3* polymorphisms has been identified. The *CYP2C8*4* variant appears to lead to reduced functional protein; however more studies are needed to show its clinical relevance.

4.2 CYP3A4

CYP3A4 is the most important enzyme of CYP450 family playing major role in the metabolism of 30% of current drugs (Zanger and Schwab 2013). It is mainly expressed in the liver and intestine (Pelkonen et al. 2008). It has a flexible and large active site and can accommodate multiple substrates (Hendrychova et al. 2011). Midazolam and testosterone are the preferable substrates for measuring *in vitro* CYP3A4 activity, whereas ketoconazole, itraconazole and troleandomycin are recommended *in vitro* inhibitors of CYP3A4 (FDA. 2011). More than 40 CYP variant alleles have been identified in *CYP3A4* but few of them have functional consequences (cypalleles.ki.se). A common variant, *CYP3A4*1B* has been associated with higher prostate tumour grade and advance prostate cancer disease. Forty six percent of patients with stage 3 or stage 4 prostate tumour carried *CYP3A4*1B*, whereas only 5% of patients with stage 1

tumour carried *CYP3A4*1B* (P < 0.001) (Rebbeck et al. 1998). An intron 6 SNP, *CYP3A4*22* (rs35599367, C>T) has been associated with reduced activity; patients carrying T allele required significantly lower statin (atorvastatin, simvastatin, or lovastatin) doses (0.2-0.6-fold, P = 0.012) than non-T carriers (Wang et al. 2011).

5. Hypothesis

It was hypothesised that *CYP2C8*3* and *CYP2C8*4* genetic polymorphisms would decrease imatinib metabolism to N-desmethyl imatinib in HLM.

6. Aims

The aims of the study were:

- To study the impact of *CYP2C8*3* and *CYP2C8*4* polymorphisms on *in vitro* metabolism of imatinib to N-desmethyl imatinib using HLMs genotyped for *CYP2C8*3* and *CYP2C8*4*, and in *CYP2C8*3/*3* pooled HLM.
- To more comprehensively characterise the kinetics of imatinib N-demethylation in HLMs and recombinant enzymes to better define kinetic parameters.
- To determine the relative contribution of CYP2C8 and CYP3A4 to imatinib N-demethylation in HLMs using specific monoclonal inhibitory antibodies and chemical inhibitors.

Chapter 2: Manuscript

This manuscript has been submitted for publication. It covers all the aims of this study apart from the impact of *CYP2C8*4* polymorphism on imatinib metabolism (discussed in chapter 3). Part of this work was previously presented at the 2014 Australasian Society of Clinical and Experimental Pharmacology and Toxicology conference (joint *ASCEPT-MPGPCR* conference), December 7-11, Melbourne, Victoria, Australia and it won the Pharmacogenomics special interest group (SIG) Award.

Title

Impact of *CYP2C8*3* polymorphism on *in-vitro* metabolism of imatinib to N-desmethyl imatinib

Muhammad Suleman Khan, Daniel T Barratt, and Andrew A Somogyi.

Discipline of Pharmacology, School of Medical Sciences (M.S.K., D.T.B., A.A.S.), and Centre for Personalised Cancer Medicine (D.T.B., A.A.S.),The University of Adelaide, South Australia, Australia; Department of Clinical Pharmacology, Royal Adelaide Hospital, Adelaide, South Australia, Australia (A.A.S.)

Running Title Page

Running Title: *CYP2C8*3* polymorphism and imatinib N-demethylation

Correspondence: Dr. Daniel Barratt

Discipline of Pharmacology, School of Medical Sciences,

Level 5, Medical School North, The University of Adelaide, South

Australia, AUSTRALIA, 5005.

Phone: +61(0)883135985 Fax: +61(0) 8 8224 0685

Email: daniel.barratt@adelaide.edu.au

Text page: 20

Table: 2

Figures: 3

References: **39** /60

Words in Abstract: 250 /250

Words in Introduction: 707 /750

Words in Discussion: 1263 /1500

Abbreviations: Cl_{int}, intrinsic clearance; HLM, human liver microsomes; HPLC, high performance liquid chromatography; K_i, substrate inhibition constant; K_m, Michaelis-Menten constant; P450, cytochrome P450; SNP, single nucleotide polymorphism; V_{max}, maximum formation rate.

Abstract

Imatinib is metabolised to N-desmethyl imatinib by CYP3A4 and CYP2C8. *In vitro* human liver microsome (HLM) studies indicate imatinib autoinhibition of CYP3A4-mediated metabolism, suggesting a more significant role for CYP2C8 on chronic dosing. Functional effects of the major *CYP2C8* polymorphism *CYP2C8*3* on N-desmethyl imatinib formation are unknown. We examined N-demethylation of imatinib in HLMs genotyped for *CYP2C8*3*, in *CYP2C8*3/*3* pooled HLMs, and in expressed CYP2C8 and CYP3A4 enzymes. Effects of CYP-selective chemical and antibody inhibitors on N-demethylation were also determined. Single enzyme Michaelis-Menten model with substrate inhibition best fitted wild-type (*CYP2C8*1/*1*) HLM (n = 5) and expressed CYP2C8 kinetic data (median ± SD K_i = 139 ± 61 µM and 149 µM, respectively). Expressed CYP3A4 showed two site enzyme kinetics with no evidence of autoinhibition. Three of four *CYP2C8*1/*3* HLMs showed single enzyme but no autoinhibition kinetics. Binding affinity was approximately 2-fold higher in *CYP2C8*1/*3* HLMs as compared to *CYP2C8*1/*1* (median ± SD K_m = 6 ± 2 *vs* 11 ± 2 µM, p=0.04). Intrinsic clearance (Cl_{int}) was higher in *CYP2C8*1/*3* HLMs compared to *CYP2C8*1/*1* (median ± SD Cl_{int} = 19 ± 8 *vs* 13 ± 2 µl/min/mg). *CYP2C8*3/*3* (pooled HLM) showed highest binding affinity (K_m = 3.6 µM) and weak autoinhibition (K_i = 449 µM) kinetics. CYP2C8 inhibitors reduced N-demethylation by 47-75%, compared to 0-30% for CYP3A4 inhibitors. These results indicate that *CYP2C8*3* may enhance CYP2C8 activity by influencing autoinhibition, and that *in vitro* the metabolism and autoinhibition of imatinib N-demethylation appears mainly mediated by CYP2C8 and not CYP3A4.

Introduction

Imatinib mesylate was the first successfully-targeted tyrosine kinase inhibitor among tyrosine kinase inhibitors (TKIs), now used as first line therapy in newly diagnosed chronic myeloid leukaemia (CML) and also used in Ph^+ acute lymphoblastic leukaemia (ALL), *c-KIT* and *PDGFR* positive gastrointestinal stromal tumor (GIST) (Linch et al. 2013;Jabbour and Kantarjian 2014;Maino et al. 2014). Treatment with imatinib is generally well tolerated, but must be continuous and indefinite for most patients to maintain disease control. Up to 50% of CML patients discontinue imatinib due to lack of efficacy or adverse effects (Gotta et al. 2014). Major determinants of resistance appear to be inadequate target site (intracellular) concentrations (Berglund et al. 2014) and mutations in the target protein (BCR-ABL)(Jabbour et al. 2013). The former is determined firstly by unbound plasma concentrations, a product of variability in metabolism, and patient compliance, and secondly by transport proteins mediating imatinib uptake into CML cells (Marin et al. 2010;Jabbour et al. 2013;Widmer et al. 2014).

Imatinib is almost completely absorbed after oral administration. Peak plasma concentrations (C_{max}) are achieved after 2-4 hours with 97 % bioavailability and half life of 18 hours (Peng et al. 2004). After oral administration approximately 65% of the systemic exposure corresponds to imatinib and 10-20% to N-desmethyl imatinib (NDIM) (Gschwind et al. 2005;Josephs et al. 2013). Imatinib is extensively metabolised in the liver and is eliminated predominantly in the feces (67% and 13% of the excreted dose in feces and urine, respectively); approximately 13% of the dose in excreta corresponds to NDIM (Gschwind et al. 2005). Several other metabolites of minor importance have also been identified (Gschwind et al. 2005;Marull and Rochat 2006;Rochat et al. 2008). A correlation between trough plasma imatinib concentrations and efficacy shows that trough total (bound plus unbound) concentrations of more than 1000 ng/ml

are associated with better outcomes (Larson et al. 2008;Picard et al. 2007;Yeung and White 2011;). Large interindividual variability exists in plasma imatinib concentrations (Bouchet et al. 2013;de Wit et al. 2015) and dosage above 600 mg is associated with adverse events (Larson et al. 2008;Widmer et al. 2014). Imatinib is metabolised to its main metabolite NDIM by CYP2C8 and CYP3A4 (Nebot et al. 2010;Filppula et al. 2013). Other CYP enzymes CYP3A5, CYP1A1, CYP1A2, CYP2D6, CYP2C9 and CYP2C19 play little or no role (Rochat et al. 2008;Filppula et al. 2013). A recent study has indicated that imatinib is an autoinhibitor of CYP3A4 metabolism *in vitro* (Filppula et al. 2012). *In silico* simulations based on these *in vitro* findings predicted that after multiple doses of imatinib (400 mg), the fraction of drug metabolised by CYP2C8 would increase from 40% to 60%, and by CYP3A4 decrease from 60% to less than 40%, due to dose and time-dependent autoinhibition of CYP3A4 activity (Filppula et al. 2013). *CYP2C8* is polymorphic and to date 16 alleles have been identified (cypalleles.ki.se). Most of the polymorphisms are not well studied and their contribution to CYP2C8 activity is variable (Zanger and Schwab 2013). *CYP2C8*3* is a common haplotype in Caucasians (11-14%) consisting of two single nucleotide polymorphisms (rs11572080 and rs10509681) that has functional consequences (Aquilante et al. 2013). *In vitro CYP2C8*3* was associated with reduced arachidonic acid and paclitaxel metabolism (Dai et al. 2001;Gao et al. 2010;Yu et al. 2013), whereas for the antidiabetic drugs repaglinide, and pioglitazone, higher activity was found for *CYP2C8*3* compared to the wild type *CYP2C8*1* enzyme (Daily and Aquilante 2009;Muschler et al. 2009;Stage et al. 2013). To date the impact of *CYP2C8*3* polymorphism on imatinib metabolism in HLM has not been investigated. Based on the previous data for CYP2C8 *in vitro* model substrate paclitaxel, we hypothesised that *CYP2C8*3* genetic polymorphism will decrease imatinib metabolism to NDIM in HLM. Therefore, we aimed to study the impact of *CYP2C8*3*

polymorphism on *in vitro* metabolism of imatinib to NDIM in HLMs genotyped for *CYP2C8*3* and in *CYP2C8*3/*3* (pooled HLM). Previous imatinib N-demethylation kinetic studies in expressed CYP2C8, CYP3A4 enzymes and HLMs had a limited number of data points; therefore we also aimed to more comprehensively characterise the kinetics of imatinib N-demethylation in HLMs and expressed enzymes to better define kinetic parameters. The relative contribution of CYP2C8 and CYP3A4 to imatinib N-desmethylation in HLMs was also studied using specific monoclonal inhibitory antibodies and chemical inhibitors.

Materials and Methods

Chemicals

Imatinib and NDIM were kindly provided by Prof Deborah White (South Australian Health and Medical Research Institute, SA, Australia). DL-Isocitric acid trisodium salt, isocitric dehydrogenase, montelukast, troleandomycin and fatty acid-free human serum albumin (HSA) were purchased from Sigma-Aldrich (Castle Hill, NSW, Australia). Disodium hydrogen orthophosphate, dipotassium hydrogen orthophosphate, magnesium chloride hexahydrate and sodium dihydrogen orthophosphate were obtained from Ajax Chemicals (Auburn, NSW, Australia). NADP-sodium salt, triethylamine and orthophosphoric acid were purchased from Merck Pty. Ltd. (Kilsyth, VIC, Australia). HPLC grade acetonitrile and methanol were purchased from Scharlau (Barcelona, Spain; distributed by Southern Cross Science Pty Ltd, Edwardstown, SA, Australia). Oligonucleotide primers and probes were purchased from Integrated DNA Technologies Pty Ltd (Baulkham Hills, NSW, Australia). iTaq Universal Probes Supermix was obtained from BioRad (Sydney, NSW, Australia). Maxwell 16 tissue DNA purification kits were purchased from Promega (Madison,WI, USA). Pierce^{TM} BCA protein assay kit was purchased from Thermo Fisher Scientific (Scoresby, VIC, Australia).

Expressed Proteins and Monoclonal Antibodies.

Human P450 isoforms (CYP3A4 and CYP2C8) co-expressed with P450 reductase and cytochrome b5 (Cyt b5) in baculovirus-infected insect cells were commercially available from Corning (Woburn, MA, USA; distributed by In-vitro Technologies Pty. Ltd, Noble Park, VIC, Australia). Monoclonal antibody inhibitors of human CYP3A4 (Falcon Gentest inhibition maB-3A4) and CYP2C8 (Falcon Gentest inhibition maB-2C8) were also obtained from Corning.

Liver Samples.

Ethical approval was obtained from University of Adelaide Ethics Committee of Human Experimentation and Human Ethics Committee of the Royal Adelaide Hospital. Human liver samples were donated by 40 patients undergoing partial hepatectomy for hepatic tumors. All liver samples were genotyped for the major *CYP2C8*3* (rs11572080 and rs10509681) single nucleotide genetic polymorphism (SNP) by assays described below, and 9 liver tissues were selected on the basis of their *CYP2C8*3* genotype. All the tissue samples used were normal based on gross morphology. Characteristics of the patients were as follows: (1) all were Caucasian; (2) ages ranged from 31 to 77 years; (3) six donors were male (HLS#14,20,26,33,34,47); 4) five patients carried *CYP2C8*1/*1* genotype and four carried *CYP2C8*1/*3* genotype. Six patients had normal clinical chemistry and hematology before surgery, HLS#20 had high concentrations of lactate dehydrogenase (3.4 x upper limit of normal). Alanine Transaminase levels were higher in HLS#20 and 44 (8 and 14 x upper limit of normal) and gamma-glutamyl transpeptidase levels were slightly higher in HLS#47 and 26 (1.5 x upper limit of normal). Albumin level was half normal in HLS#44. All tissue samples were frozen in liquid nitrogen and stored at -80°C until used. *CYP2C8*3/*3* pooled HLM were purchased from Corning (Woburn, MA, US).

***CYP2C8* Genotyping**:

Genomic DNA was isolated from liver tissues using Promega Maxwell 16 instrument (Madison, WI) with Maxwell 16 Tissue DNA purification kit according to the manufacturer's protocol. *CYP2C8*3* genotype was determined by allelic discrimination assay using custom designed primers and probes at final concentrations of 6 µM each, 1 x iTaq Universal Probes Supermix and 20 ng of DNA (20 µl reaction volume) on a CFX96 real-time PCR system (BioRad, Sydney,

NSW, Australia). Primer and probe sequences are listed in the Table 1. Thermocycling conditions were 95^{o}C for 3 minutes then 39 cycles of 95^{o}C for 5 seconds and 65^{o}C for 30 seconds, with allelic discrimination performed using CFX Manager 3.0 software (BioRad) after 39 cycles. Sequenced genotype controls (*CYP2C8*1/*1, *1/*3, *3/*3*) and two non-template controls were included in every run of assays.

Enzyme Kinetics in HLMs:

HLMs were prepared from human liver bank samples using a previously described differential centrifugation method (Zanger et al. 1988) and used by us previously (Li et al. 2013). Total microsomal protein content was quantified by BCA assay according to the manufacturer's protocol (Pierce Biotechnology, Inc.).

NDIM formation from imatinib in HLMs was performed as follows (n = 1 for all incubation conditions in each HLM, pooled HLM or recombinant enzyme experiment). All incubations were performed at 37°C in a shaking water bath. Incubation medium, in a final volume of 100 µl, consisted of 50 µg HLM protein, NADPH regenerating system (1 mM NADP, 1 unit/ml isocitrate dehydrogenase, 5 mM DL-isocitric acid, 5 mM magnesium chloride), and 0.1 mM of disodium phosphate buffer (pH 7.4). After a 3-minute preincubation, the reaction was initiated by the addition of various concentrations of imatinib (20 concentrations, final concentration range 1 to 200 µM imatinib), and terminated by the addition of 50 µl of ice cold acetonitrile after 60 minutes incubation. Fifty microgram HLM protein and 60 minutes incubation time were chosen based on preliminary experiments (data not shown).The mixture was then centrifuged at 21000 xg at 4^{o}C for 10 min and 40 µl of the supernatant was injected for high-performance liquid chromatography (HPLC) analysis. For *CYP2C8*3/*3* (pooled HLM), imatinib concentrations up to 500 µM were required to estimate K_i. Stock solutions of imatinib were

prepared in milli Q water. Working standards of imatinib were prepared in phosphate buffer (pH = 7.4) and 10 µl of the working standard was added to the incubation to obtain the final imatinib concentration. Controls consisting of phosphate buffer, HLM, and imatinib without NADPH regenerating system were included in each run.

Imatinib non-specific binding to 50 µg HLM protein was determined by an ultrafiltration method using centrifree devices (Merck Millipore Ltd., Cork, Ireland). Samples and devices were equilibrated at 37^{o}C before application. The device was first pre-washed with 1 ml of phosphate buffer. Fifty microlitres of sample was then added to the device, centrifuged at 2000 xg for 20 min at 37^{o}C, and the ultrafiltrate discarded. One hundred and fifty microlitres of the sample was then added to the device and centrifuged at 2000 xg for 20 min at 37^{o}C. To 50 µl of filtrate, 25 µl ice cold acetonitrile was added and centrifuged at 21000 xg at 4^{o}C for 10 min and 40 µl was injected for HPLC analysis.

Since fatty acids from microsomes can inhibit CYP2C8 activity, we also studied the effect of fatty-acid free HSA 2% w/v (sequesters fatty acids) on NDIM formation (Wattanachai et al. 2011). The binding of imatinib to HSA 2% w/v and HLM was studied using ultrafiltration as above. The effect on NDIM formation was studied using final imatinib concentrations of 5, 10 and 20 µM in incubations without HSA, and 8.5, 17 and 34 µM in incubations with HSA to account for binding of imatinib to HSA. To determine total NDIM formation, incubations were performed in duplicate as above. After 60 minutes the samples were pooled and placed on ice to stop the reaction. Twenty five microlitres of pooled sample was added to another tube containing 37.5 µl of ice cold acetonitrile and placed on ice for 10 min. The samples were then centrifuged at 21000 xg at 4^{o}C for 10 min. To 31.2 µl supernatant, 25 µl phosphate buffer was added and 40 µl was injected for HPLC analysis to quantify total NDIM. The rest of the pooled sample

underwent ultrafiltration as above. To filtrate 1.5 x volume ice cold acetonitrile was added and placed on ice for 10 min. The samples were then centrifuged at 21000 xg at 4^{o}C for 10 min. To 31.2 µl supernatant, 25 µl phosphate buffer was added and 40 µl was injected for HPLC analysis to quantify unbound imatinib concentrations. Total NDIM formation and unbound imatinib was quantified using HPLC assay described below with slight modifications. For unbound imatinib, standards for the imatinib calibration curve were diluted in phosphate buffer and underwent the same ultrafiltration process as samples. NDIM standards were prepared using the same dilutions as were used in incubation with HSA.

Enzyme Kinetics in cDNA-Expressed P450 Enzymes:

Expressed CYP2C8 and CYP3A4 (final concentrations of 54 pmol/ml and 20 pmol/ml respectively) were incubated at substrate concentrations and conditions identical to those used for HLMs.

Inhibition Studies with Chemical Inhibitors:

The effects of chemical inhibitors of CYP3A4 (troleandomycin, 25 µM) and CYP2C8 (montelukast, 10 µM) on NDIM formation was investigated using imatinib concentrations equivalent to the respective K_m values for each HLM, *CYP2C8*3/*3* (pooled HLM), and expressed enzymes. For *CYP2C8*3/*3* (pooled HLM), 10 µM imatinib was also investigated to enable the quantification of NDIM formation in the presence of inhibitors. Stock solutions of troleandomycin were prepared in methanol. Working standards were prepared in 0.1M sodium phosphate buffer (pH 7.4), with a 0.7% final concentration of methanol in the incubation medium. Stock solutions of montelukast were prepared in milli Q water. All components of the incubation medium except imatinib were preincubated with troleandomycin or methanol control for 20 min, or with montelukast or water control for 3 min, at 37°C. The reaction was then

initiated by the addition of substrate and terminated after 60 minutes incubation. NDIM formation was quantified using the HPLC assay as described below.

Inhibition Studies with Monoclonal Antibodies against P450s:

Monoclonal antibodies against CYP3A4 (Falcon Gentest inhibition maB-3A4, MAB3A4) and CYP2C8 (Falcon Gentest inhibition maB-2C8, MAB-2C8) were used in accordance with the manufacturer's recommendations. Antibodies (10 µl of 4mg/ml MAB-3A4 or 2.5 mg/ml MAB-2C8 in 25mM Tris buffer, pH 7.5) or inhibitor-free controls (10 µl 25mM Tris buffer,pH 7.5) were pre-incubated with an incubation medium containing 50 µg HLMs, NADPH-regenerating system, incubation buffer, and 25 mM Tris buffer (pH 7.5) on ice for 20 minutes. The reaction was then initiated by the addition of imatinib concentrations equivalent to the K_m values of each HLM and *CYP2C8*3/*3* (pooled HLM). For *CYP2C8*3/*3* (pooled HLM), 10 µM imatinib was also investigated to enable the quantification of NDIM formation in the presence of MAB-2C8. The reaction was terminated after 60 minutes incubation.

HPLC Conditions:

NDIM formation was quantified using an HPLC assay with UV detection that was modified from a previously reported method (Tan et al. 2011). In brief, separation of imatinib, NDIM and two unidentified minor metabolites (M1 and M2), was achieved on a 5 µm C18 reverse-phase column (150 x 2 mm; LUNA; Phenomenex, Torrance, CA, USA) using a mobile phase of 15% (v/v) acetonitrile and 0.4% triethylamine in 0.02 mM dipotassium phosphate buffer (pH 3), and a flow rate of 0.55 ml/min. The column was protected by a 4 x 2 mm C18 security guard cartridge (Phenomenex). Analytes were detected at 235 nm. The peak area was calculated using Shimadzu Class-VP software (version 6.12, SP2; Shimadzu, Kyoto, Japan). The retention times for imatinib, NDIM, M1 and M2 were 12.5, 8.5, 6.3 and 18 minutes, respectively. Calibration curves

comprised six standards of NDIM over the concentration range of 0.25–10 µM. Stock solutions of NDIM were prepared in milli Q water. Working standards for the calibration curve were prepared in phosphate buffer (pH 7.4). Working standards were then diluted in disodium phosphate buffer containing 50 µg of albumin (in place of the NADPH regenerating system and microsomes) to a final volume of 100 µl to replicate incubation samples. Fifty microlitres of ice cold acetonitrile was added before centrifuging at 21000 xg at 4^{o}C for 10 min. Forty microlitres of the supernatant was then injected for HPLC analysis.

Inter and intra-assay variabilities were determined using the analysis of quality-control NDIM samples at three different concentrations: low (0.75 µM), medium (2 µM), and high (4 µM). Intra-assay variability was calculated from six replicates of each quality control on a single assay run. Inter-assay variability was calculated from duplicate quality control samples on six different days. Inter and intra-assay inaccuracy for quality control samples was less than 8% and 5%, respectively. Precision calculated as co-efficient of variation (CV) was less than 8% (inter-assay) and 6% (intra-assay).

Data Analysis:

NDIM formation rate was calculated using the following equation:

Formation rate (V) = NDIM concentration (pmol/µl) x incubation volume (µl)/HLM protein (µg) /total incubation time (min) (1)

The assessment of the kinetic data was initially performed by Eadie-Hofstee plots [V/substrate concentration(S) versus V] which directed the choice of kinetic models to be tested. The following models for each HLM and expressed enzyme were fitted to the kinetic data:

One-enzyme (Michaelis-Menten) model

$$v = V_{max} * [S] / (K_m + [S]) \quad (2)$$

One-enzyme (Michaelis-Menten) model with substrate inhibition

$$v = V_{max}*[S]/ (K_m + [S]*(1+[S]/K_i)) \quad (3)$$

Two-enzyme (Michaelis-Menten) model

$$v = (V_{max1}*[S]/ (K_{m1}+[S])) + (V_{max2}*[S]/ (K_{m2}+[S])) \quad (4)$$

Two-enzyme (Michaelis-Menten) model with one enzyme substrate inhibition

$$v = (V_{max1}*[S]/ (K_{m1}+[S])) + (V_{max2}*[S]/ (K_{m2} + [S]*(1+[S]/K_i))) \quad (5)$$

Two-enzyme (Michaelis-Menten) model with two-enzyme substrate inhibition

$$v = (V_{max1}*[S]/ K_{m1}+ [S]*(1+[S]/K_{i1})) + (V_{max2}*[S]/ (K_{m2} + [S]*(1+[S]/K_{i2}))) \quad (6)$$

Sigmoidal model with substrate inhibition

$$v = (V_{max}*[S]^h/ (K_m{}^h + [S]^h)) +V_{max}*[S]/ (K_m+ [S]*(1+[S]/K_i))) \quad (7)$$

Where K_m is substrate concentration [S] at which half of the V_{max} is obtained, V_{max} is the maximum formation rate, K_i substrate inhibition constant and h is the Hill slope. The criteria for selection of the best model for analysis was based on visual inspection of the Eadie-Hofstee plot, extra sum of squares F-test and comparisons of goodness of fit of different models to the observed kinetic data. Kinetic parameters (K_m, $V_{max,}$ K_i and Hill slope) were estimated using GraphPad Prism 5 software (San Diego, CA). Intrinsic clearance (Cl_{int}) was calculated as V_{max}/K_m. Inhibition data were expressed as a percentage of the corresponding non-inhibitor

controls. Mann Whitney U test was used for statistical comparison between two genotype groups (*CYP2C8*1/*1* and *CYP2C8*1/*3*).

Results:

Enzyme Kinetics in cDNA-Expressed P450 Enzymes:

Figure 1 shows the Enzyme kinetics of NDIM formation in expressed CYP2C8 and CYP3A4 enzymes. A single enzyme Michaelis-Menten model with substrate inhibition best fitted the expressed CYP2C8 kinetic data (Figure 1A and 1B). Eadie-Hofstee plot suggested a two site interaction for expressed CYP3A4 (Figure 1C) and so a two enzyme Michaelis-Menten model best fitted the expressed CYP3A4 kinetic data (Figure 1D). The estimated values of kinetic parameters (V_{max}, K_m, K_i and Cl_{int}) for CYP2C8 and for the CYP3A4 low-affinity/high-capacity (V_{max1}, K_{m1}, and Cl_{int1}) and the high-affinity/low-capacity site (V_{max2}, K_{m2}, and Cl_{int2}) are listed in Table 2. Two unidentified peaks M1 and M2 were found in expressed CYP3A4 but not in CYP2C8 (data not shown).

Enzyme Kinetics in HLMs:

Enzyme kinetic parameters of NDIM formation in HLMs with *CYP2C8*1/*1* (n=5), *CYP2C8*1/*3* (n=4) and *CYP2C8*3/*3* (pooled HLM) genotypes are listed in Table 2. Eadie-Hofstee plots for all *CYP2C8*1/*1* HLMs indicated one enzyme with substrate inhibition and a single enzyme Michaelis-Menten model with substrate inhibition provided the best fit to the kinetic data. Representative Eadie-Hofstee and Michaelis-Menten plots for *CYP2C8*1/*1* HLM are shown in Figure 2A and 2B, respectively. No autoinhibition was found in three out of four HLMs with *CYP2C8*1/*3* genotypes. The Eadie-Hofstee plot was linear for these HLMs, indicating single enzyme kinetics. One *CYP2C8*1/*3* (HLS#26) displayed atypical kinetics: a sigmoidal model with substrate inhibition provided the best fit to the kinetic data (Supplementary

Figure 2). Representative Eadie-Hofstee and Michaelis-Menten plots for *CYP2C8*1/*3* HLMs are shown in Figure 2C and 2D, respectively. Eadie-Hofstee plot for *CYP2C8*3/*3* (pooled HLM) indicated autoinhibition (Fig 2E). A single enzyme Michaelis-Menten model with substrate inhibition provided best fit to the kinetic data (Fig 2F). Binding affinity was approximately 2-fold higher for *CYP2C8*1/*3* HLMs as compared to *CYP2C8*1/*1* HLMs (median K_m = 6 *vs* 11, P=0.04). *CYP2C8*3/*3* pooled HLM displayed the highest binding affinity (K_m = 3.6 µM). Cl_{int} was also higher in HLMs with *CYP2C8*1/*3* as compared to *CYP2C8*1/*1* HLMs (median Cl_{int} = 19 *vs* 13 µl/min/mg), but the difference was significant (P = 0.02) only if HLS#26 was excluded from analysis due to atypical enzyme kinetics. Kinetics of NDIM formation in the presence of fatty acid free HSA (2% w/v) remained unchanged (data not shown). Approximately 15% of imatinib was bound to 50 µg HLM protein.

Inhibition studies

Figure 3 shows the effects of CYP2C8 and CYP3A4 chemical (montelukast and troleandomycin respectively) and monoclonal antibody inhibitors on NDIM formation in expressed CYP2C8 and CYP3A4, and HLMs with *CYP2C8*1/*1* (n=5), *CYP2C8*1/*3* (n=4), *CYP2C8*3/*3* (pooled HLM) genotypes. Montelukast and MAB-2C8 inhibited NDIM formation by at least 65% (NDIM below LOQ) and 78%, respectively, in expressed CYP2C8; montelukast inhibited NDIM formation with a median of 70% and 61%, and MAB-2C8 by a median of 50% and 47% in *CYP2C8*1/*1* and *CYP2C8*1/*3* HLMs, respectively. Troleandomycin inhibited NDIM formation by 58%, and by a median of 21% and 14%, in expressed CYP3A4, *CYP2C8*1/*1* HLM and *CYP2C8*1/*3* HLM, respectively. MAB-3A4 inhibited 42% and less than 10% of NDIM formation in expressed CYP3A4, and *CYP2C8*1/*1* and *CYP2C8*1/*3* HLM, respectively. Using 4 µM imatinib (~K_m) for *CYP2C8*3/*3* (pooled HLM) NDIM formation was

below the limit of quantification after montelukast and MAB-2C8 inhibition. Using a higher imatinib concentration of 10 µM for *CYP2C8*3/*3* (pooled HLM), montelukast, MAB-2C8, troleandomycin and MAB-3A4 inhibited 45%, 30%, 22% and 15% of NDIM formation, respectively. CYP2C8 chemical and antibody inhibitors inhibited NDIM formation in CYP3A4 expressed enzyme by less than 10%, whereas no effect of CYP3A4 inhibitors (chemical and antibody) was found in expressed CYP2C8. No difference was found in NDIM formation inhibition when montelukast was preincubated for 20 min with HLM in the presence of NADPH-regeneration system as compared to 3 min preincubation (data not shown).

Discussion

To our knowledge this study reports for the first time the impact of *CYP2C8*3* genetic polymorphisms on *in vitro* metabolism of imatinib to NDIM. This study also shows the concentration-dependent autoinhibition of NDIM formation in human liver microsomes, and that the autoinhibition of the NDIM formation was primarily mediated by CYP2C8 and not CYP3A4 as shown by the expressed enzyme kinetics data.

A significant finding from this study is that the *CYP2C8*3* polymorphism appears to alter autoinhibition of NDIM formation in HLMs. All 5 *CYP2C8*1/*1* HLMs showed autoinhibition, whereas three out of four *CYP2C8*1/*3* HLMs showed no autoinhibition. This is similar to a previous study that investigated the impact of *CYP2C8*3* polymorphism on inhibition of paclitaxel 6α- hydroxylation. Troglitazone and raloxifine IC_{50} values were increased by 2.4- and 4.2-fold in *CYP2C8*1/*3* compared to wild type *CYP2C8*1/*1* expressed enzymes (Gao et al. 2010), suggesting a significant reduction in the *in vitro* inhibitory effects for *CYP2C8*1/*3* polymorphism. Our results show that the imatinib binding affinity of *CYP2C8*1/*3* HLMs was almost 2-fold higher (median K_m 6 *vs* 11 µM) than *CYP2C8*1/*1* HLMs; and Cl_{int} was also significantly higher for *CYP2C8*1/*3* HLMs as compared to *CYP2C8*1/*1* HLMs (median Cl_{int} = 19 *vs* 13 µl/min/mg), only if one HLS#26 was excluded from analysis due to atypical enzyme kinetics (Supplementary Figure 2). *CYP2C8*3/*3* (pooled HLM) showed 3-fold reduced autoinhibition (K_i = 449 *vs* 139 µM) and 3-fold higher binding affinity compared to *CYP2C8*1/*1* (3.6 *vs* 11 µM). These results suggests that *CYP2C8*3* is a gain-of-function genotype for imatinib N-demethylation as measured by high Cl_{int} and this was due to a higher binding affinity (K_m) and no autoinhibition.

Three of 5 *CYP2C8*1/*1* HLMs had abnormal clinical chemistry or haematology prior to surgery, possibly indicating abnormal liver function, however their NDIM formation kinetics where not obviously different from the other *CYP2C8*1/*1* HLMs and therefore are unlikely to confound genotype comparisons.

The functional consequences of *CYP2C8*3* polymorphism are variable and appear substrate specific. Our hypothesis was based on *in-vitro* studies that showed significantly lower activity for *CYP2C8*3* towards the model substrate paclitaxel (Dai et al. 2001;Gao et al. 2010;Yu et al. 2013); however our findings are similar to higher activity found for other CYP2C8 substrates such as repaglinide, rosiglitazone and pioglitazone (Daily and Aquilante 2009;Muschler et al. 2009;Yu et al. 2013). For pioglitazone metabolism to the M-IV metabolite, Cl_{int} was found higher in HLMs with **3/*3* genotype as compared to wild type (35 ± 9 *vs* 24 ± 4 pmol/min/mg/µM) (Muschler et al. 2009). Interestingly concentration-dependent autoinhibition of M-IV formation was also found in this study. For repaglinide, expressed *CYP2C8*3* variant showed 1.31-fold higher Cl_{int} than the *CYP2C8*1* enzyme (Yu et al. 2013). Clinical studies have also shown higher activity for *CYP2C8*3* genotype. For repaglinide, mean area under the plasma concentration-time curve (AUC) and C_{max} were 45% and 39% lower, respectively, in subjects with **1/*3* genotype as compared to wild type (Niemi et al. 2003). For rosiglitazone, trough plasma concentrations were significantly lower in **1/*3* than the wild type (23.1 v 16.5 ng/ml) (Stage et al. 2013). Similarly for pioglitazone AUC was decreased by 34% and 26% in **3/*3* and **1/*3* subjects, respectively (Tornio et al. 2008). All these studies indicate that *CYP2C8*3* polymorphism leads to enhanced activity for some substrates and our findings for imatinib N-demethylation are supportive.

The exact mechanism for substrate-specific effects of *CYP2C8*3* is unknown. CYP2C8 has a large active site with multiple binding sites (Schoch et al. 2008), which may partly explain the gain-of-function for *CYP2C8*3* variants for relatively smaller substrates such as pioglitazone (356 g/mol) rosiglitazone (357 g/mol), repaglinide (453 g/mol) and likely imatinib as well (493 g/mol), compared to reduced function for the larger substrate paclitaxel (854 g/mol). *CYP2C8*3* consists of two non-synonymous SNPs (R139K, K399R), however the effect of *CYP2C8*3* on protein conformation and imatinib-CYP2C8 interactions are not yet characterized. Whilst *CYP2C8*3* is in strong linkage with *CYP2C9*2* (Muschler et al. 2009), no contribution of CYP2C9 was found in imatinib metabolism (Filppula et al. 2013).

We found two site enzyme kinetics and no evidence of autoinhibition in expressed CYP3A4. Our data support previous finding that indicated a non-linear Eadie-Hofstee plot for NDIM formation in expressed CYP3A4, albeit with few data points (n = 5) and forced through a linear model (Rochat et al. 2008). From another previous study similarly limited by fewer data points (Nebot et al. 2010), and from Filppula et al. (2013), we have extracted data from their kinetic analysis and also found non-linear Eadie-Hofstee plots indicating at least two site enzyme kinetics (Supplementary Figure 1). Atypical enzyme kinetics have been reported for other CYP3A4 substrates as well (Houston and Kenworthy 2000;Klees et al. 2005), which may result from interaction between several binding sites within CYP3A4's large active site (Houston and Galetin 2005).

Our original hypothesis was based on the autoinhibition of NDIM formation in expressed CYP3A4 as shown by Filppula and colleagues 2013. However, this was based on limited data points with the K_i estimate of 1400 µM approximately 4.5-fold higher than the maximum substrate concentration used (320 µM) (Filppula et al. 2013). Imatinib is a mechanism-based

inhibitor of midazolam 1′-hydroxylation (Filppula et al. 2012). However, whilst we lack experiments in our study under mechanism-based inhibition conditions, our kinetic data in expressed CYP3A4 found no concentration-dependent autoinhibition of NDIM formation. The reason for this discrepancy is unclear and may result from multiple site interactions on the large CYP3A4 active site as evident from our expressed CYP3A4 kinetic data. We have also observed two unidentified metabolites M1 and M2 in accordance with previous studies (Gschwind et al. 2005;van Erp et al. 2007;Rochat et al. 2008;Filppula et al. 2013). These peaks were observed in both HLM and expressed CYP3A4, however they were absent in expressed CYP2C8. This supports previous *in vitro* findings that CYP3A4 is a major contributor to the formation of these metabolites, whereas CYP2C8 mainly contributes to NDIM formation (Filppula et al. 2013).

We demonstrated clear autoinhibition of NDIM formation in expressed CYP2C8, in accordance with (Filppula et al. 2013). However, in that study the estimated K_i was 2.6-fold higher (395 µM versus 149 µM) and greater than the maximum substrate concentration used (320 µM). This difference might be due to the shorter incubation time used (4 min *vs* 60 min). At such a short incubation time the reaction may not reach full equilibrium, and there is a possibility of underestimating the mechanism-based inhibition involved. We also repeated kinetic experiments for expressed CYP2C8 and CYP3A4 using 10 min incubation and found that the kinetics of both CYP2C8 and CYP3A4 remained unchanged (data not shown). Similar to our findings, substrate inhibition was also found for another CYP2C8 substrate, pioglitazone (Tornio et al. 2008;Muschler et al. 2009), however the exact mechanism of CYP2C8-mediated autoinhibition is unknown and needs further investigation. The inhibition experiments carried out using chemical and specific monoclonal antibody inhibitors showed that CYP2C8 is likely the major enzyme involved in NDIM formation in HLM. This study has some limitations of using small

number of samples and we were not able to find any *CYP2C8*3/**3 homozygous variant in our human liver bank for comparison within our samples. We also lack total CYP450 content and CYP2C8 and CYP3A4 protein expression data in HLMs, which could further clarify the mechanism such as impact of *CYP2C8*3* on CYP2C8 protein expression and contribution of CYP3A4.

In conclusion we have shown for the first time the autoinhibition of NDIM formation in HLMs. Also autoinhibition of NDIM formation was influenced by *CYP2C8*3* genotype, which was associated with high substrate-enzyme binding affinity. We also found that autoinhibition is mediated by the CYP2C8 enzyme not CYP3A4, and that CYP2C8 is likely the major enzyme involved in NDIM formation. This warrants clinical investigations of the impact of *CYP2C8* genotype on imatinib plasma concentration and possible drug-drug interactions with other CYP2C8 substrates.

Acknowledgment

We thank Yibai Li for technical assistance with the HPLC analysis and microsomes preparation.

Authorship Contributions

Participated in Research Design: Khan, Barratt and Somogyi

Conducted experiments: Khan

Performed data analysis: Khan, Barratt and Somogyi

Wrote or contributed to the writing of the manuscript: Khan, Barratt and Somogyi

References

Aquilante, C. L., M. Niemi, L. Gong, R. B. Altman and T. E. Klein (2013). PharmGKB summary: very important pharmacogene information for cytochrome P450, family 2, subfamily C, polypeptide 8. Pharmacogenet Genomics **23**(12): 721-728.

Berglund, E., S. J. Ubhayasekera, F. Karlsson, P. Akcakaya, W. Aluthgedara, J. Ahlen, R. Frobom, I. L. Nilsson, W. O. Lui, C. Larsson, J. Zedenius, J. Bergquist and R. Branstrom (2014). Intracellular concentration of the tyrosine kinase inhibitor imatinib in gastrointestinal stromal tumor cells. Anticancer Drugs **25**(4): 415-422.

Bouchet, S., K. Titier, N. Moore, R. Lassalle, B. Ambrosino, S. Poulette, P. Schuld, C. Belanger, F. X. Mahon and M. Molimard (2013). Therapeutic drug monitoring of imatinib in chronic myeloid leukemia: experience from 1216 patients at a centralized laboratory. Fundam Clin Pharmacol **27**(6): 690-697.

Dai, D., D. C. Zeldin, J. A. Blaisdell, B. Chanas, S. J. Coulter, B. I. Ghanayem and J. A. Goldstein (2001). Polymorphisms in human CYP2C8 decrease metabolism of the anticancer drug paclitaxel and arachidonic acid. Pharmacogenetics **11**(7): 597-607.

Daily, E. B. and C. L. Aquilante (2009). Cytochrome P450 2C8 pharmacogenetics: a review of clinical studies. Pharmacogenomics **10**(9): 1489-1510.

de Wit, D., H. J. Guchelaar, J. den Hartigh, H. Gelderblom and N. P. van Erp (2015). Individualized dosing of tyrosine kinase inhibitors: are we there yet? Drug Discov Today **20**(1): 18-36.

Filppula, A. M., J. Laitila, P. J. Neuvonen and J. T. Backman (2012). Potent mechanism-based inhibition of CYP3A4 by imatinib explains its liability to interact with CYP3A4 substrates. Br J Pharmacol **165**(8): 2787-2798.

Filppula, A. M., M. Neuvonen, J. Laitila, P. J. Neuvonen and J. T. Backman (2013). Autoinhibition of CYP3A4 leads to important role of CYP2C8 in imatinib metabolism: variability in CYP2C8 activity may alter plasma concentrations and response. Drug Metab Dispos **41**(1): 50-59.

Gao, Y., D. Liu, H. Wang, J. Zhu and C. Chen (2010). Functional characterization of five CYP2C8 variants and prediction of CYP2C8 genotype-dependent effects on in vitro and in vivo drug-drug interactions. Xenobiotica **40**(7): 467-475.

Gotta, V., S. Bouchet, N. Widmer, P. Schuld, L. A. Decosterd, T. Buclin, F. X. Mahon, C. Csajka and M. Molimard (2014). Large-scale imatinib dose-concentration-effect study in CML patients under routine care conditions. Leuk Res **38**(7): 764-772.

Gschwind, H. P., U. Pfaar, F. Waldmeier, M. Zollinger, C. Sayer, P. Zbinden, M. Hayes, R. Pokorny, M. Seiberling, M. Ben-Am, B. Peng and G. Gross (2005). Metabolism and disposition of imatinib mesylate in healthy volunteers. Drug Metab Dispos **33**(10): 1503-1512.
Houston, J. B. and A. Galetin (2005). Modelling atypical CYP3A4 kinetics: principles and pragmatism. Arch Biochem Biophys **433**(2): 351-360.

Houston, J. B. and K. E. Kenworthy (2000). In vitro-in vivo scaling of CYP kinetic data not consistent with the classical Michaelis-Menten model. Drug Metab Dispos **28**(3): 246-254.
Jabbour, E. and H. Kantarjian (2014). Chronic myeloid leukemia: 2014 update on diagnosis, monitoring, and management. Am J Hematol **89**(5): 547-556.

Jabbour, E. J., J. E. Cortes and H. M. Kantarjian (2013). Resistance to tyrosine kinase inhibition therapy for chronic myelogenous leukemia: a clinical perspective and emerging treatment options. Clin Lymphoma Myeloma Leuk **13**(5): 515-529.

Josephs, D. H., D. S. Fisher, J. Spicer and R. J. Flanagan (2013). Clinical pharmacokinetics of tyrosine kinase inhibitors: implications for therapeutic drug monitoring. Ther Drug Monit **35**(5): 562-587.

Kirchheiner, J., I. Meineke, U. Fuhr, C. Rodriguez-Antona, E. Lebedeva and J. Brockmoller (2008). Impact of genetic polymorphisms in CYP2C8 and rosiglitazone intake on the urinary excretion of dihydroxyeicosatrienoic acids. Pharmacogenomics **9**(3): 277-288.

Klees, T. M., P. Sheffels, O. Dale and E. D. Kharasch (2005). Metabolism of alfentanil by cytochrome p4503a (cyp3a) enzymes. Drug Metab Dispos **33**(3): 303-311.

Larson, R. A., B. J. Druker, F. Guilhot, S. G. O'Brien, G. J. Riviere, T. Krahnke, I. Gathmann and Y. Wang (2008). Imatinib pharmacokinetics and its correlation with response and safety in chronic-phase chronic myeloid leukemia: a subanalysis of the IRIS study. Blood **111**(8): 4022-4028.

Li, Y., J. K. Coller, M. R. Hutchinson, K. Klein, U. M. Zanger, N. J. Stanley, A. D. Abell and A. A. Somogyi (2013). The CYP2B6*6 allele significantly alters the N-demethylation of ketamine enantiomers in vitro. Drug Metab Dispos **41**(6): 1264-1272.

Linch, M., J. Claus and C. Benson (2013). Update on imatinib for gastrointestinal stromal tumors: duration of treatment. Onco Targets Ther **6**: 1011-1023.

Maino, E., R. Sancetta, P. Viero, S. Imbergamo, A. M. Scattolin, M. Vespignani and R. Bassan (2014). Current and future management of Ph/BCR-ABL positive ALL. Expert Rev Anticancer Ther **14**(6): 723-740.

Marin, D., A. Bazeos, F. X. Mahon, L. Eliasson, D. Milojkovic, M. Bua, J. F. Apperley, R. Szydlo, R. Desai, K. Kozlowski, C. Paliompeis, V. Latham, L. Foroni, M. Molimard, A. Reid, K. Rezvani, H. de Lavallade, C. Guallar, J. Goldman and J. S. Khorashad (2010). Adherence is the

critical factor for achieving molecular responses in patients with chronic myeloid leukemia who achieve complete cytogenetic responses on imatinib. J Clin Oncol **28**(14): 2381-2388.

Marull, M. and B. Rochat (2006). Fragmentation study of imatinib and characterization of new imatinib metabolites by liquid chromatography-triple-quadrupole and linear ion trap mass spectrometers. J Mass Spectrom **41**(3): 390-404.

Muschler, E., J. Lal, A. Jetter, A. Rattay, U. Zanger, G. Zadoyan, U. Fuhr and J. Kirchheiner (2009). The role of human CYP2C8 and CYP2C9 variants in pioglitazone metabolism in vitro. Basic Clin Pharmacol Toxicol **105**(6): 374-379.

Nebot, N., S. Crettol, F. d'Esposito, B. Tattam, D. E. Hibbs and M. Murray (2010). Participation of CYP2C8 and CYP3A4 in the N-demethylation of imatinib in human hepatic microsomes. Br J Pharmacol **161**(5): 1059-1069.

Niemi, M., J. B. Leathart, M. Neuvonen, J. T. Backman, A. K. Daly and P. J. Neuvonen (2003). Polymorphism in CYP2C8 is associated with reduced plasma concentrations of repaglinide. Clin Pharmacol Ther **74**(4): 380-387.

Peng, B., C. Dutreix, G. Mehring, M. J. Hayes, M. Ben-Am, M. Seiberling, R. Pokorny, R. Capdeville and P. Lloyd (2004). Absolute bioavailability of imatinib (Glivec) orally versus intravenous infusion. J Clin Pharmacol **44**(2): 158-162.

Picard, S., K. Titier, G. Etienne, E. Teilhet, D. Ducint, M. A. Bernard, R. Lassalle, G. Marit, J. Reiffers, B. Begaud, N. Moore, M. Molimard and F. X. Mahon (2007). Trough imatinib plasma levels are associated with both cytogenetic and molecular responses to standard-dose imatinib in chronic myeloid leukemia. Blood **109**(8): 3496-3499.

Rochat, B., V. Zoete, A. Grosdidier, S. von Grunigen, M. Marull and O. Michielin (2008). In vitro biotransformation of imatinib by the tumor expressed CYP1A1 and CYP1B1. Biopharm Drug Dispos **29**(2): 103-118.

Schoch, G. A., J. K. Yano, S. Sansen, P. M. Dansette, C. D. Stout and E. F. Johnson (2008). Determinants of cytochrome P450 2C8 substrate binding: structures of complexes with montelukast, troglitazone, felodipine, and 9-cis-retinoic acid. J Biol Chem **283**(25): 17227-17237.

Stage, T. B., M. M. Christensen, S. Feddersen, H. Beck-Nielsen and K. Brosen (2013). The role of genetic variants in CYP2C8, LPIN1, PPARGC1A and PPARgamma on the trough steady-state plasma concentrations of rosiglitazone and on glycosylated haemoglobin A1c in type 2 diabetes. Pharmacogenet Genomics **23**(4): 219-227.

Tan, K. L., R. Ankathil and S. H. Gan (2011). Method development and validation for the simultaneous determination of imatinib mesylate and N-desmethyl imatinib using rapid resolution high performance liquid chromatography coupled with UV-detection. J Chromatogr B Analyt Technol Biomed Life Sci **879**(30): 3583-3591.

Tornio, A., M. Niemi, P. J. Neuvonen and J. T. Backman (2008). Trimethoprim and the CYP2C8*3 allele have opposite effects on the pharmacokinetics of pioglitazone. Drug Metab Dispos **36**(1): 73-80.

van Erp, N. P., H. Gelderblom, M. O. Karlsson, J. Li, M. Zhao, J. Ouwerkerk, J. W. Nortier, H. J. Guchelaar, S. D. Baker and A. Sparreboom (2007). Influence of CYP3A4 inhibition on the steady-state pharmacokinetics of imatinib. Clin Cancer Res **13**(24): 7394-7400.

Wattanachai, N., T. M. Polasek, T. M. Heath, V. Uchaipichat, W. Tassaneeyakul, W. Tassaneeyakul and J. O. Miners (2011). In vitro-in vivo extrapolation of CYP2C8-catalyzed paclitaxel 6alpha-hydroxylation: effects of albumin on in vitro kinetic parameters and assessment of interindividual variability in predicted clearance. Eur J Clin Pharmacol **67**(8): 815-824.

Widmer, N., C. Bardin, E. Chatelut, A. Paci, J. Beijnen, D. Leveque, G. Veal and A. Astier (2014). Review of therapeutic drug monitoring of anticancer drugs part two--targeted therapies. Eur J Cancer **50**(12): 2020-2036.

Yeung, D. T. and D. L. White (2011). Imatinib trough levels in chronic myelogenous leukemia: does one dose fit all? Leuk Lymphoma **52**(2): 165-167.

Yu, L., D. Shi, L. Ma, Q. Zhou and S. Zeng (2013). Influence of CYP2C8 polymorphisms on the hydroxylation metabolism of paclitaxel, repaglinide and ibuprofen enantiomers in vitro. Biopharm Drug Dispos **34**(5): 278-287.

Zanger, U. M. and M. Schwab (2013). Cytochrome P450 enzymes in drug metabolism: regulation of gene expression, enzyme activities, and impact of genetic variation. Pharmacol Ther **138**(1): 103-141.

Zanger, U. M., F. Vilbois, J. P. Hardwick and U. A. Meyer (1988). Absence of hepatic cytochrome P450bufI causes genetically deficient debrisoquine oxidation in man. Biochemistry **27**(15): 5447-5454.

Foot note:

This work was supported by the University of Adelaide, School of Medical Sciences funding, and The University of Adelaide International Post Graduate Research Scholarship.

Part of this work was previously presented at the following conference: M S Khan (2014) Impact of *CYP2C8*1/*3* polymorphism on *in-vitro* metabolism of imatinib to its active metabolite N-desmethyl imatinib. Joint *ASCEPT-MPGPCR* 2014 conference; 2014 December 7-11, Melbourne, Victoria, Australia.

Figure Legends

Figure I

Eadie-Hofstee [V/S *vs* V] and Michaelis-Menten plots [V/S] of N-desmethyl imatinib formation in insect cell-expressed CYP2C8 and CYP3A4 enzymes. (A) Eadie-Hofstee plot indicating single enzyme autoinhibition in expressed CYP2C8. (B) Single enzyme Michaelis-Menten model with substrate inhibition best fit of expressed CYP2C8 kinetic data. (C) Eadie-Hofstee plot indicating two site interaction for expressed CYP3A4. (D) Two enzyme Michaelis-Menten model best fit of expressed CYP3A4 kinetic data.

Figure II

Representative Eadie-Hofstee [V/S *vs* V] and Michaelis-Menten plots [V/S] of N-desmethyl imatinib formation in *CYP2C8*1/*1,*1/*3* and **3/*3* (pooled HLM). (A) Eadie-Hofstee plot for *CYP2C8*1/*1* HLM indicating single enzyme with substrate inhibition. (B) Single enzyme Michaelis-Menten model with substrate inhibition best fit of *CYP2C8*1/*1* HLM kinetic data. (C) Eadie-Hofstee plot for *CYP2C8*1/*3* HLM indicating single enzyme with no substrate inhibition. (D) Single enzyme Michaelis-Menten model best fit of *CYP2C8*1/*3* HLM kinetic data. (E) Eadie-Hofstee plot for *CYP2C8*3/*3* pooled HLM indicating single enzyme with substrate inhibition. (F) Single enzyme Michaelis-Menten model with substrate inhibition best fit of *CYP2C8*3/*3* pooled HLM kinetic data.

Figure III

Effect of CYP2C8 and CYP3A4 chemical inhibitors (montelukast and troleandomycin, respectively), and monoclonal antibodies against CYP2C8 (MAB-2C8) and CYP3A4 (MAB-3A4), on N-desmethyl imatinib formation in HLMs with *CYP2C8*1/*1* (n=5), *CYP2C8*1/*3* (n=4) and *CYP2C8*3/*3* (pooled HLM). The substrate concentration was equivalent to the

relative K_m values of each HLM (Table 2) except for *CYP2C8*3/*3* (pooled HLM), 10 µM imatinib was used. MAB-2C8 and montelukast were tested against CYP3A4 and MAB-3A4 and trolendomycin were tested against CYP2C8 for specificity. Data are presented as median with error bar indicating standard deviation. X- * NDIM formed after inhibition by montelukast and MAB-2C8 in expressed CYP2C8 was below the limit of quantification, therefore minimum inhibition is presented in the figure.

Table 1

CYP2C8 genotype	Forward primer sequence	Reverse primer sequence
*CYP2C8*3* (rs11572080)	5′-CACAACCTTGCGGAATTTTGG-3′	5′-AGGCAGTGAGCTTCCTCTTG-3′
*CYP2C8*3* (rs10509681)	5′-GAAAGTGGCCAGGGTCAAAG-3′	5′-TGTTACTTCCAGGGCACAAC-3′
Probe sequences	wild type probe	Variant probe
*CYP2C8*3* (rs11572080)	5′-/56-FAM/TCCTCAATGCT+C+T+TCTTCCCCA/3IABkFQ/3′	5′-/5HEX/TCCTCAATGCT+C+C+TCTTCCCCA/3IABkFQ/3′
*CYP2C8*3* (rs10509681)	5′-/56-FAM/AAATTC+T+C+T+GTCATCATGTAGCACG/3IABkFQ/-3′	5′-/5HEX/AAATTC+T+T+T+GTCATCATGTA GCACG/3IABkFQ/3′

FAM: 6-carboxy-fluorescein; HEX: hexachloro-6-carboxy-fluorescein; 3IABkFQ: 3′lowa Black FQ quencher. "+" precedes locked nucleic acid bases

Table 2

Enzyme kinetic parameters of N-desmethyl imatinib formation in expressed CYP2C8 and CYP3A4 enzymes, and in HLMs with *CYP2C8*1/*1* (n=5), *CYP2C8*1/*3* (n=4) and *CYP2C8*3/*3* (pooled HLM) genotype.

CYP2C8			V_{max} (SE)	K_m (SE)	K_i (SE)	Cl_{int}
			(pmol/min/pmol P450)	(µM)	(µM)	(µl/min/pmol)
			0.6 (0.04)	5 (1.2)	149 (35)	0.12
CYP3A4	K_{m1} (SE)	V_{max1} (SE)	Cl_{int1}	K_{m2} (SE)	V_{max2} (SE)	Cl_{int2}
	26 (8.6)	1(0.1)	0.3	0.4 (0.4)	0.4 (0.1)	1
**1/*1*			V_{max} (SE)	K_m (SE)	K_i (SE)	Cl_{int}
			(pmol/min/mg)	(µM)	(µM)	(µl/min/mg)
HLS #20			133 (5.7)	9 (0.8)	111 (12)	15
HLS #33			140 (17.3)	11 (2.7)	107 (30)	13
HLS #44			153 (17)	12 (2.7)	250 (92)	13
HLS #46			63 (5.7)	7 (1.5)	139 (34)	9
HLS #47			142 (10.3)	13 (1.9)	197	11
Median ± SD			140 ± 36	11 ± 2	139 ± 61	13 ± 2
**1/*3*						
HLS #14			126 (2.6)	7 (0.7)	NA	18
HLS #24			111 (2.1)	5 (0.5)	NA	22
HLS #34			56 (1.2)	3 (0.4)	NA	19
Median ± SD (excluding HLS#26)			111 ± 37	5 ± 2*	NA	19 ± 2*

HLS #26^	37 (6.3)	8 (1.1)	40 (50)	5
Median ± SD (all **1/*3*)	84 ± 43	6 ± 2*	NA	19 ± 8
**3/*3*				
Pooled HLM	22 (0.7)	4 (0.6)	449 (57)	6

*Mann-Whitney U test P<0.05 versus **1/*1*. ^ Sigmoidal model with substrate inhibition provided best fit (Hill slope value h = 4). V_{max}: maximum rate of formation, K_m: concentration at which half of the V_{max} is obtained, Cl_{int}: intrinsic clearance calculated as V_{max}/K_m, K_i: substrate inhibition constant. K_{m1} and V_{max1} is a low affinity and high capacity site. K_{m2} and V_{max2} is a high affinity and low capacity site. SE: Standard Error. No substrate inhibition was found in three out of four *CYP2C8*1/*3* HLMs and a single enzyme Michaelis-Menten model best fitted to the kinetic data. Statistics with and without HLS#26 presented in table.

Figure 1

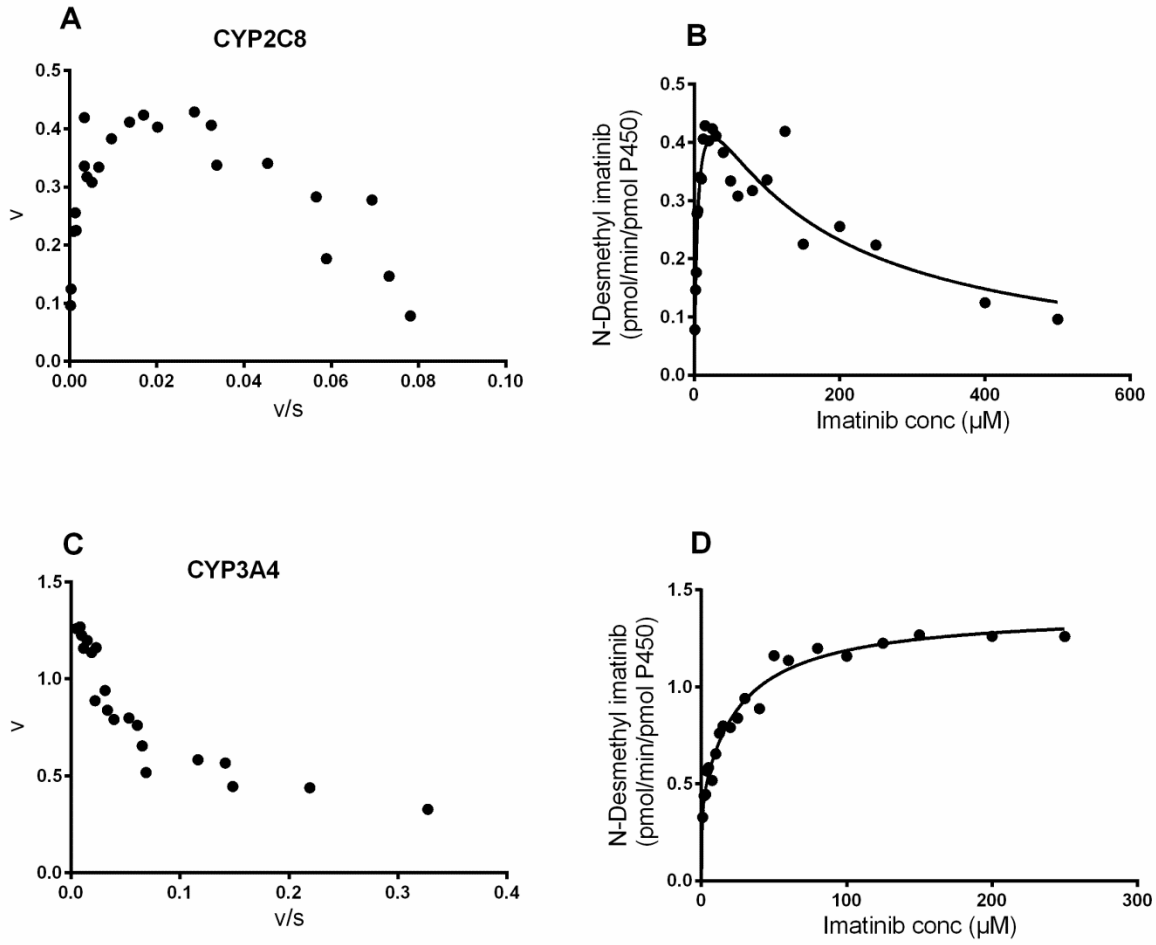
A
CYP2C8
v
v/s
0.0
0.1
0.2
0.3
0.4
0.5
0.00
0.02
0.04
0.06
0.08
0.10
B
N-Desmethyl imatinib
(pmol/min/pmol P450)
Imatinib conc (μM)
0
200
400
600
C
CYP3A4
1.0
1.5
0.1
0.2
0.3
0.4
D
100
300

Figure 2

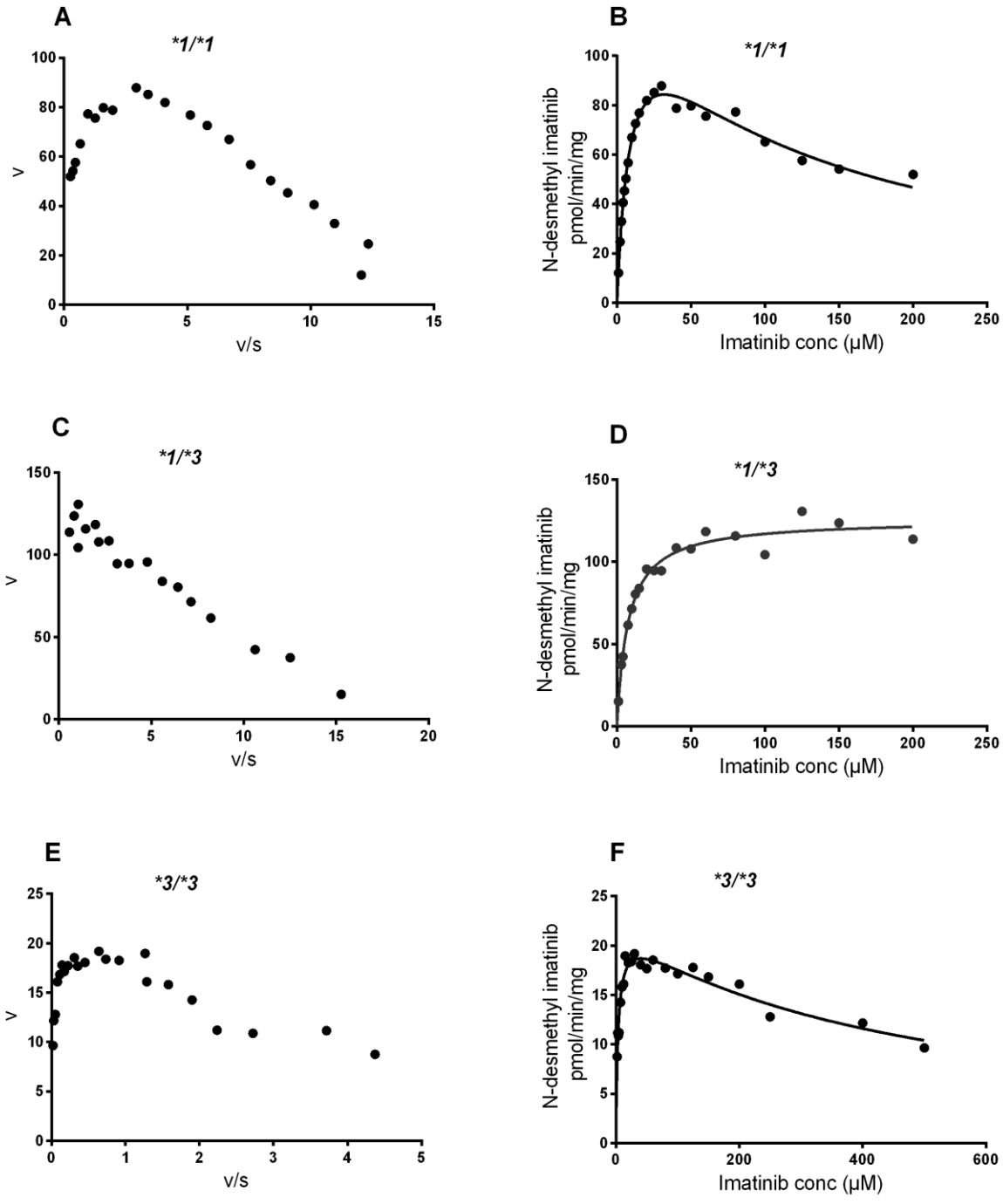
A
*1/*1
v
v/s
B
*1/*1
N-desmethyl imatinib pmol/min/mg
Imatinib conc (μM)
C
*1/*3
v
v/s
D
*1/*3
N-desmethyl imatinib pmol/min/mg
Imatinib conc (μM)
E
*3/*3
v
v/s
F
*3/*3
N-desmethyl imatinib pmol/min/mg
Imatinib conc (μM)

Figure 3

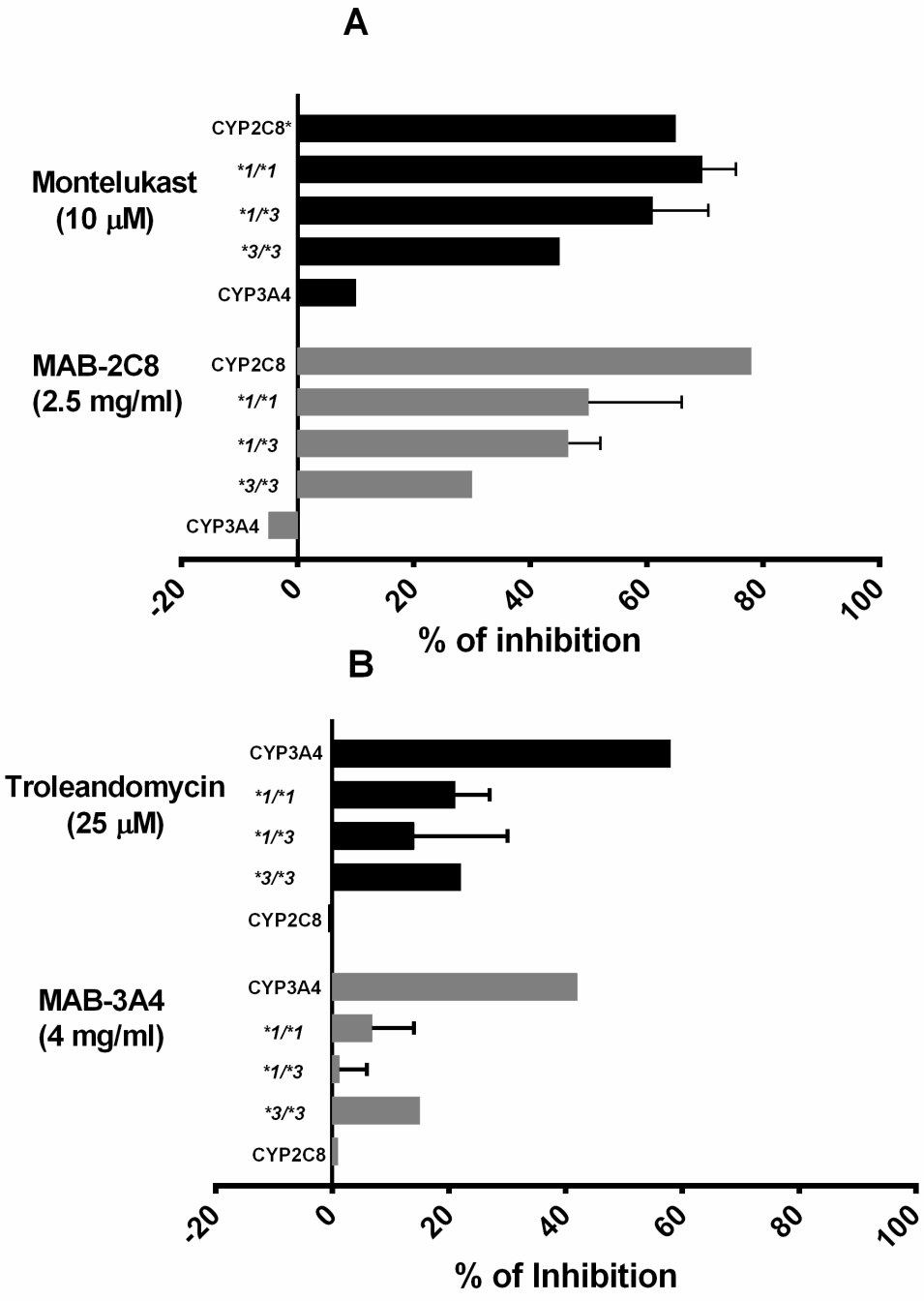
A
Montelukast
(10 μM)
CYP2C8*
*1/*1
*1/*3
*3/*3
CYP3A4
MAB-2C8
(2.5 mg/ml)
CYP2C8
*1/*1
*1/*3
*3/*3
CYP3A4
-20
0
20
40
60
80
100
% of inhibition
B
Troleandomycin
(25 μM)
CYP3A4
*1/*1
*1/*3
*3/*3
CYP2C8
MAB-3A4
(4 mg/ml)
CYP3A4
*1/*1
*1/*3
*3/*3
CYP2C8
-20
0
20
40
60
80
100
% of Inhibition

Supplementary Figure 1

Eadie-Hofstee plots [V/S vs V] of N-desmethyimatinib formation in expressed CYP3A4 enzyme. (A) Approximate data was extracted from the expressed CYP3A4 enzyme kinetic data as shown by (Nebot et al., 2010). (B) and (Flippula et al., 2013), see reference below. A non-linear Eadie-Hofstee plot suggesting involvement of at least two sites.

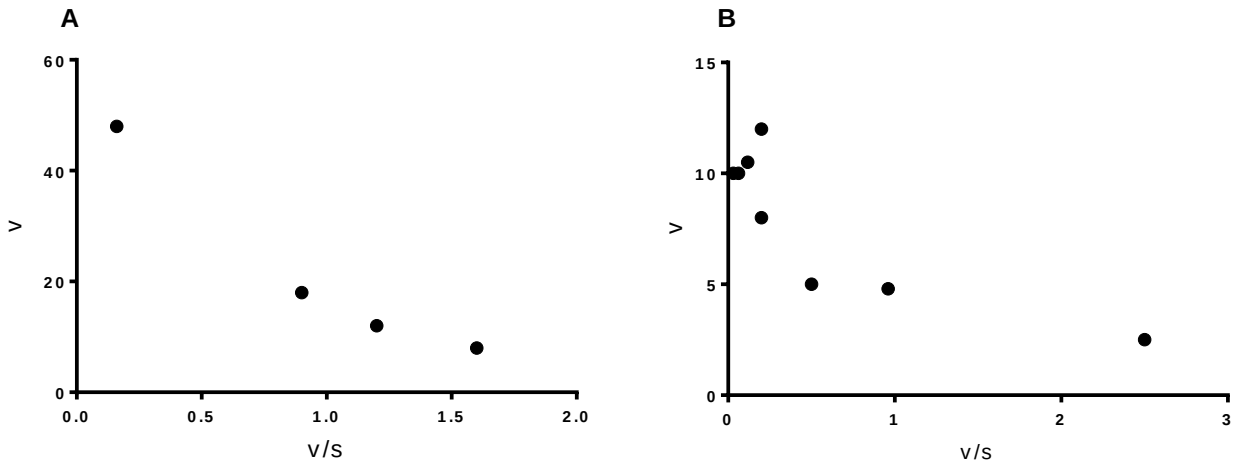

1. Nebot, N., S. Crettol, F. d'Esposito, B. Tattam, D. E. Hibbs and M. Murray (2010). "Participation of CYP2C8 and CYP3A4 in the N-demethylation of imatinib in human hepatic microsomes." Br J Pharmacol **161**(5): 1059-1069.

2. Filppula, A. M., M. Neuvonen, J. Laitila, P. J. Neuvonen and J. T. Backman (2013). "Autoinhibition of CYP3A4 leads to important role of CYP2C8 in imatinib metabolism: variability in CYP2C8 activity may alter plasma concentrations and response." Drug Metab Dispos **41**(1): 50-59.

Supplementary Figure 2

Sigmoidal plot with one enzyme substrate inhibition and Eadie-Hofstee [V/S *vs* V] plots of N-desmethyl imatinib formation in HLS# 26.

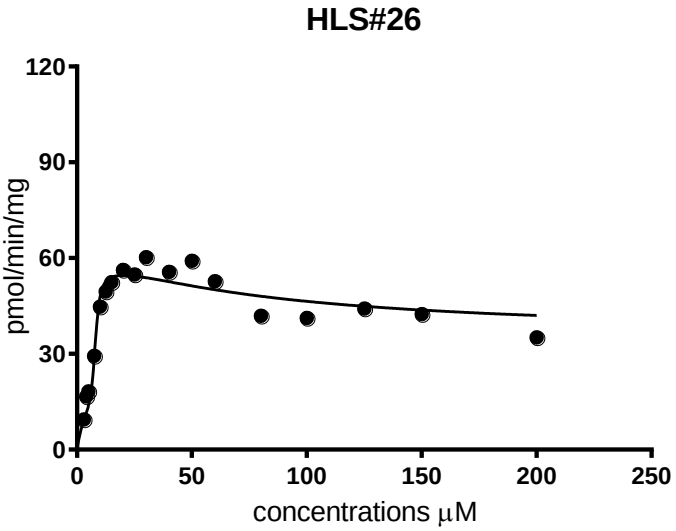

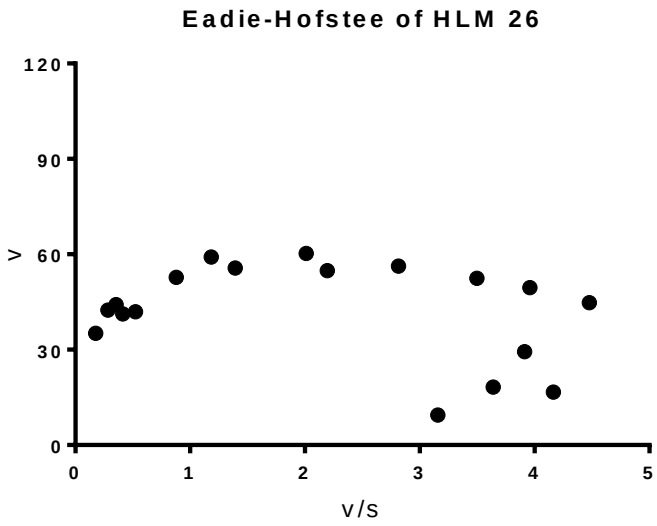

Chapter 3: Supplementary Studies

Impact of *CYP2C8*4* on imatinib metabolism to NDIM and qualitative description of two unidentified metabolites M1 and M2.

Introduction

In addition to the impact of *CYP2C8*3* on imatinib metabolism (Chapter 2) the following supplementary studies, investigating the impact of *CYP2C8*4* on imatinib metabolism and qualitative description of unidentified metabolites M1 and M2 are described here.

*CYP2C8*4* enzyme kinetics and inhibition studies

*CYP2C8*4* (rs1058930) polymorphism is found only in Caucasians with an allele frequency of 7-8% (Bahadur et al. 2002; Aquilante et al. 2013a). Studies on *CYP2C8*4* are limited, but it appears to be associated with lower activity. For paclitaxel, lower activity was found in *CYP2C8*4* HLMs and expressed *CYP2C8*4* variants as compared to the wild type (Bahadur et al. 2002;Gao et al. 2010;Jiang et al. 2011). Similarly lower activity was also found for other substrates such as amodiaquine and fluoxetine N-demethylation (Gao et al. 2010;Wang et al. 2014b). Functional consequences of *CYP2C8*4* on imatinib metabolism have not been investigated as yet. Based on previous studies it was hypothesised that *CYP2C8*4* will decrease imatinib metabolism to N-desmethyl imatinib in HLMs.

Qualitative analysis of unknown imatinib metabolites

Imatinib is metabolised to its main metabolite N-desmethyl imatinib by CYP2C8 and CYP3A4 (Nebot et al. 2010;Filppula et al. 2013a). In addition to N-desmethyl imatinib, several other metabolites are also found, that include oxidative products and glucuronides (Gschwind et al. 2005;Marull and Rochat 2006;Rochat et al. 2008;Filppula et al. 2013a). CYP3A4 contribution to

these metabolites is greater (1:3), which includes the further metabolism of N-desmethyl imatinib, whereas CYP2C8 metabolism is primarily to N-desmethyl imatinib (Filppula et al. 2013a). The exact role of these metabolites in imatinib metabolism has not yet been investigated due to lack of authentic standards. Qualitative analysis of two unidentified metabolites M1 and M2 identified in the HLM and expressed enzyme experiments is described here.

Methods

*CYP2C8*4* genotyping, enzyme kinetics and inhibition studies

*CYP2C8*4* genotypes were determined by allelic discrimination assay as described in Chapter 2. Primer and probe sequences were as follows. The forward primer 5'-CCCAGGAACTCACAACAAAGTG-3' and the reverse primer 5'-GTTGCTAATATCTTACCTGCTCCA-3', wild type probe 5'-/56-FAM/CCTCGGGACTTTA+T+C+GATTGCT/3IABkFQ/-3', and the variant probe 5'-/5HEX/CCTCGGGACTTTA+T+G+GATTGCT/3IABkFQ/3'. Sequenced genotype controls (*CYP2C8*1/*1*, **1/*4* and **4/*4*) and two no-template controls were included in every run of the assay. Two liver tissues were selected for microsomal extraction on the basis of their **4* genotype. Both patients were Caucasian males with the **1/*4* genotype. Liver tissues used were normal based on gross morphology. HLMs were prepared from the two livers as described previously (Zanger et al. 1988). Enzyme kinetics and inhibition experiments were performed following the same procedure as described in chapter two. Model selection criteria were as described in chapter two.

Qualitative analysis of unknown imatinib metabolites

Peak areas for two unidentified peaks M1 and M2 were monitored at their respective retention times (Figure 3.1) and used for qualitative description of kinetics and inhibition of M1 and M2 formation in the HLM and recombinant enzymes, experiments described in Chapter 2.

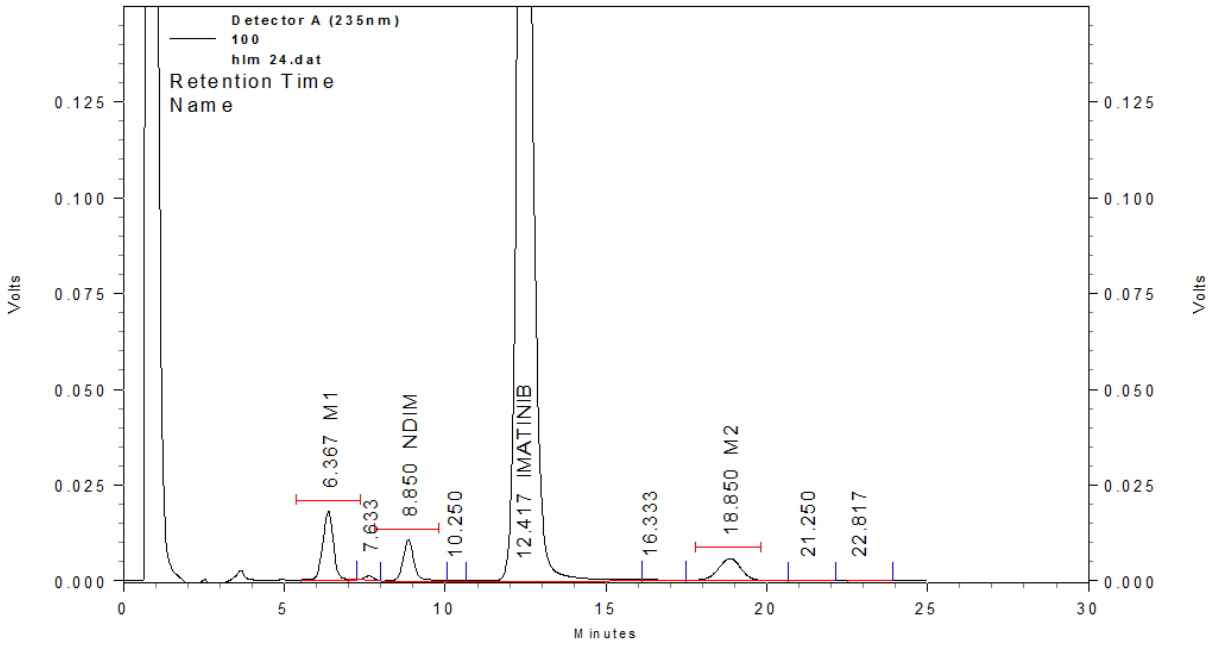

Figure 3.1: Representative chromatogram of imatinib, N-desmethyl imatinib and two unidentified metabolites M1 and M2.

Results and Discussion

*CYP2C8*4* enzyme kinetics and inhibition studies

Enzyme kinetic parameters for one *CYP2C8*1/*4* were not calculated due to minimum activity (N-desmethyl imatinib below LOQ). For the other *CYP2C8*1/*4*, Eadie-Hofstee plot indicated one enzyme with substrate inhibition. A single enzyme Michaelis-Menten model with substrate inhibition provided the best fit to the kinetic data. Eadie-Hofstee and Michaelis-Menten plots are shown in Figure 3.2A and 3.2B, respectively.

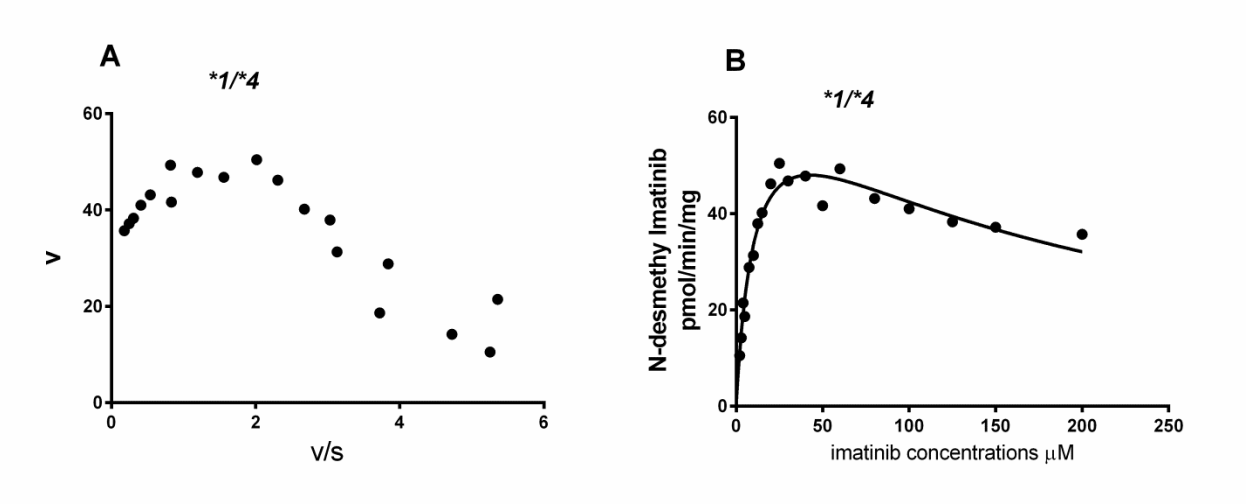

Figure 3.2. Eadie-Hofstee [V/S *vs* V] and Michaelis-Menten plots [V/S] for N-desmethyl imatinib formation from imatinib in *CYP2C8*1/*4* HLM. (A) Eadie-Hofstee plot indicating single enzyme with substrate inhibition. (B) Single enzyme Michaelis-Menten model with substrate inhibition best fit of *CYP2C8*1/*4* HLM kinetic data.

Estimated kinetic parameters were as follows: K_m was 11 µM (95% CI, 7-15), V_{max} was 73 pmol/min/mg (95% CI, 61-86), intrinsic clearance ($Cl_{int} = V_{max}/ K_m$) was 7 µl/min/mg, and K_i was 163 µM (95% CI, 89-237).

Using 10 µM imatinib (~K_m) for *CYP2C8*1/*4* HLM, N-desmethyl imatinib formation was below the limit of quantification after montelukast and CYP2C8 monoclonal inhibitory antibody (MAB-2C8) inhibition. At higher substrate concentrations (15 µM), montelukast and MAB-2C8 inhibited 60% and 54% of N-desmethyl imatinib formation, respectively, whereas no inhibition was found after the CYP3A4 monoclonal inhibitory antibody (MAB-3A4) and troleandomycin inhibition (Figure 3.3). Montelukast and MAB-2C8 inhibited N-desmethyl imatinib formation by at least 65% (N-desmethyl imatinib formation below LOQ) and 78%, respectively, in

recombinant CYP2C8. Troleandomycin and MAB-3A4 inhibited N-desmethyl imatinib formation by 58% and 42%, respectively, in recombinant CYP3A4.

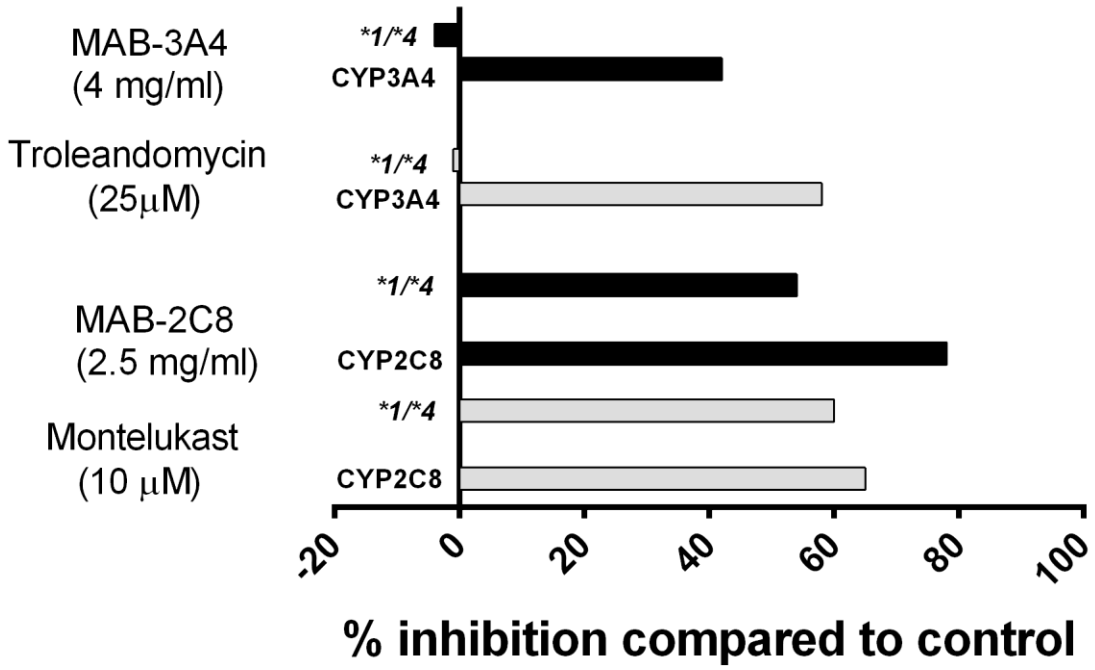

Figure 3.3. Effect of CYP3A4 and CYP2C8 chemical inhibitors (troleandomycin and montelukast, respectively), and monoclonal antibodies against CYP3A4 (MAB-3A4) and CYP2C8 (MAB-2C8), on N-desmethyl imatinib formation in HLMs with *CYP2C8*1/*4* (n=1) and recombinant CYP3A4 and CYP2C8 enzyme.

Compared to the wild type *CYP2C8*1/*1* data described in chapter two, *CYP2C8*1/*4* appears to result in lower activity for imatinib N-demethylation. This was indicated by the lack of activity in one HLM, and for another HLM lower intrinsic clearance was found (CL_{int} = 7 *vs* 11±2 µl/min/mg) due to 2-fold lower catalytic activity (V_{max}) compared to the wild type (V_{max} = 73 *vs* 140±31 pmol/min/mg). Binding affinity and inhibitory constant (K_i) were comparable to *CYP2C8*1/*1* HLMs (11 vs 11± 2 µM) and (163 vs 139 ± 61 µM), respectively. These data are in accordance with the previous studies, which have shown greatly reduced catalytic activity associated with *CYP2C8*4* variant. Only 15% paclitaxel 6α-hydroxylation activity was found in

expressed *CYP2C8*1/*4* variant compared to the wild type (Singh et al. 2008). Similarly paclitaxel CL_{int} was 3-fold lower in *CYP2C8*4* expressed variant in yeast cell compared to the wild type, due to low catalytic activity (V_{max}), $P < 0.01$ (Gao et al. 2010). Studies have also shown reduced expression of CYP2C8 protein associated with the *CYP2C8*4* variant (Singh et al. 2008;Gao et al. 2010), whereas other studies have shown no effect on protein expression (Wang et al. 2014b). Structure-function studies have shown that the *CYP2C8*4* variant changes the secondary and tertiary structure of CYP2C8, resulting in a reduced function protein as shown by *CYP2C8*4* inactive CYP-420 state (Jiang et al. 2011). The inactive CYP-420 form was also found in *CYP2C8*4* variant expressed in bacterial cells (Singh et al. 2008). These results indicate that *CYP2C8*4* is loss-of-function allele. Previously the impact of *CYP2C8*4* variant on imatinib had not been investigated. The results from this preliminary study show that *CYP2C8*4* appears to be a reduced function allele for imatinib N-demethylation. However this needs validation in larger number of samples and expressed variants.

Qualitative analysis of unknown imatinib metabolites

In HLMs, imatinib was also converted to two unidentified metabolites with a retention time of 6.4 min, called M1, and at a retention time of 18.8 min, called M2 (Figure 3.1). Compared to N-desmethyl imatinib formation which showed substrate-dependent autoinhibition, peak areas for M1 and M2 increased with increase in substrate concentration with no evidence of concentration-dependent reduction, as shown in Figure 3.4; this assumes linear M1 and M2 concentration-peak area relationships. M1 and M2 peak areas increased with increase in imatinib concentrations.

Based on the retention times, M1 appears to be the oxidative metabolite AFN911, whereas M2 could be CGP72383 or CGP71422, as described previously (Gschwind et al. 2005). These results

are in accordance with previous studies which showed that imatinib Phase I metabolism pathways included N-demethylation (main metabolite), and other pathways such as piperazine ring oxidation with lactam formation, benzyl hydroxylation (AFN911) and piperazine-N-4 oxidation (CGP71422), or pyridine N-oxidation (CGP72383) (Gschwind et al. 2005).

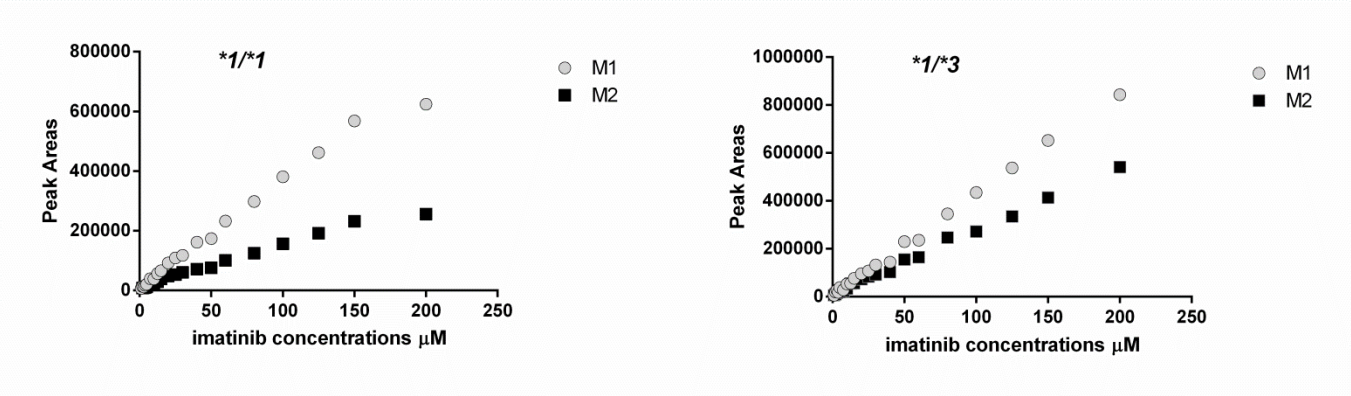

Figure 3.4: Formation of unidentified peaks M1 and M2 from imatinib in HLMs with **1/*1* and **1/*3* genotype.

In vitro metabolism studies in recombinant CYP3A4 and CYP2C8 showed that CYP3A4 appears to be the main enzyme contributing to the formation of M1 and M2, in accordance with the previous study (Filppula et al. 2013a). M1 and M2 peaks were found only in recombinant CYP3A4, whereas no peaks were found in recombinant CYP2C8. As shown in Figure 3.5, using MAB-2C8, no M2 inhibition was found in HLMs, whereas M1 formation (assessed by peak areas) appears to be enhanced, suggesting a shift of metabolic pathway as a result of CYP2C8 inhibition. MAB-3A4 inhibited both M1 and M2 by 50% and 38%, respectively in recombinant CYP3A4, whereas in all HLMs both M1 and M2 were inhibited by approximately 15-20%.

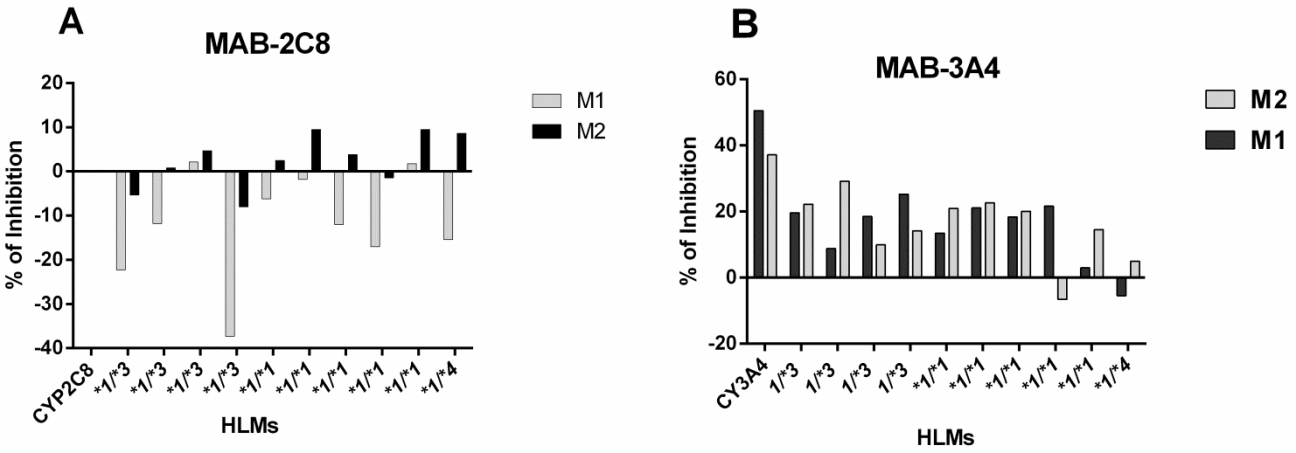

Figure 3.5: Effect of CYP2C8 and CYP3A4 monoclonal antibodies against CYP3A4 (MAB-3A4) and CYP2C8 (MAB-2C8), on M1 and M2 formation in all human liver microsomes and recombinant CYP2C8 and CYP3A4 enzymes. (A) M1 and M2 peaks were absent in recombinant CYP2C8, therefore no data are presented. M1 peak area increased, whereas no M2 inhibition was found after MAB-2C8 inhibition. (B) M1 and M2 inhibition after MAB-3A4 inhibition.

Chapter 4: Discussion and future directions

A major finding from this study is that the *CYP2C8*3* polymorphism appears to alter the autoinhibition of NDIM formation in HLM. Autoinhibition was found in all *CYP2C8*1/*1* HLMs, whereas no autoinhibition was detected in three out of four *CYP2C8*1/*3* HLMs. *CYP2C8*3/*3* pooled HLM (obtained commercially) also showed very weak autoinhibition. This finding provides the first evidence that imatinib CYP2C8-mediated autoinhibition of N-desmethyl imatinib formation is genotype dependent. However, clinical consequences of CYP2C8-mediated autoinhibition have not been investigated as yet.

Previously, the functional consequences of *CYP2C8*3* and *CYP2C8*4* genetic polymorphisms on imatinib metabolism were unknown. In this study *CYP2C8*3* appears to lead to enhanced activity for *in vitro* imatinib metabolism to N-desmethyl imatinib. This supports previous findings that *CYP2C8*3* is a gain-of-function genotype for some substrates such as some antidiabetic agents. The functional consequences of *CYP2C8*4* are inconclusive as data were available from only one HLM. However, the result supported previous findings of loss-of-function associated with *CYP2C8*4* polymorphism. These findings could be valuable in explaining individual differences in imatinib pharmacokinetics and provide information for individualised dosing.

This study could have been improved by measurements of the protein contents for CYP2C8 and CYP3A4 in HLMs that would have helped to determine their relative contribution to overall activity. *CYP2C8*3* and *CYP2C8*4* genotype effect on expression could also be investigated by comparing protein contents between the CYP2C8 wild type and variant HLMs. In addition, determination of the total P450 content in HLMs would provide an estimate of the catalytic

efficiency of the microsomes, which may help to explain the *CYP2C8*1/*4* HLM deficient in catalytic activity.

CYP3A4 polymorphisms are also a confounding factor, for example the *CYP3A4*22* polymorphism is associated with reduced activity (Wang et al. 2011), that might contribute to the overall metabolism (CL_{int}) in HLMs. Therefore data on *CYP3A4* polymorphism would help in identifying such an effect. A Previous study has reported that recombinant CYP3A5 catalyses imatinib N-demethylation with a similar affinity as CYP3A4 (44 and 43 µM respectively) (Nebot et al. 2010). However, recently recombinant CYP3A5 was shown to have a minor effect on imatinib depletion, with an estimated contribution of less than 1% to the total hepatic clearance via the N-demethylation pathway (Filppula et al. 2013a). Therefore the contribution of CYP3A5 was not investigated in this study.

This study has an advantage over previous *in vitro* studies of using a large number of kinetic data points. This enabled a better characterisation of kinetic parameters, and detection of atypical kinetics such as substrate inhibition and two site interactions. This study demonstrated clear autoinhibition of N-desmethyl imatinib formation in the recombinant CYP2C8 enzyme. Similar to our finding, substrate inhibition was also found for another CYP2C8 substrate, pioglitazone (Tornio et al. 2008;Muschler et al. 2009). The mechanism of CYP2C8-mediated autoinhibition for CYP2C8 substrates has not been investigated as yet.

A previous study has reported autoinhibition of NDIM formation in recombinant CYP3A4 (Filppula et al. 2013). However the estimated Ki value (1400 µM) was ~ 4.5-fold greater than the maximum substrate concentration used (320µM). Our kinetic data in recombinant CYP3A4 found two site enzyme kinetics with no evidence of autoinhibition of NDIM formation. The

reason for this finding of two site enzyme kinetics is unclear but may result from substrate specific multiple site interactions on the large CYP3A4 active site (Houston and Galetin 2005), as evident from recombinant CYP3A4 kinetic data in this study.

Future directions

To confirm lack of autoinhibition of N-desmethyl imatinib formation in *CYP2C8*1/*3* genotype, the results from this study need validation in expressed *CYP2C8*1/*1*, *CYP2C8*1/*3* and *CYP2C8*3/*3* variants, and also in HLMs using more clinically relevant concentrations. The potential *in vivo* consequences of these findings may be predicted using *in silico* simulations.

To further clarify if CYP2C8 autoinhibition is caused by imatinib or N-desmethyl imatinib. HLMs and recombinant CYP2C8 enzymes could be pre incubated with deuterated N-desmethyl imatinib as an inhibitor of CYP2C8 activity. A LC-MS detection method would help to differentiate between actual N-desmethyl imatinib formations in incubations and deuterated N-desmethyl imatinib. The estimation of kinetic parameters such as K_m, V_{max} and CL_{int} for N-desmethyl imatinib formation with and without deuterated N-desmethyl imatinib pre incubation would help in detecting inhibitory effects of N-desmethyl imatinib. In addition, investigation is needed to characterise the *in vitro* inhibitory effects (such as IC_{50} values, time dependent inhibition) of imatinib and N-desmethyl imatinib on CYP2C8 activity in HLM and in recombinant enzymes using CYP2C8 marker reactions such as paclitaxel 6α-hydroxylation and rosiglitazone para-hydroxylation. Furthermore, it will be of interest to investigate if these *in vitro* inhibitory effects of imatinib or N-desmethyl imatinib are *CYP2C8*3* genotype-dependent.

It may be hypothesised that imatinib CYP3A4 inhibitory effects are substrate specific. It would be of interest to test this hypothesis by investigating inhibitory effects of imatinib on CYP3A4 by using multiple marker substrates for CYP3A4 activity.

*CYP2C8*3* gain-of-function for imatinib N-demethylation and *CYP2C8*4* associated reduced activity needs validation in expressed *CYP2C8*3* and *CYP2C8*4* variants. In addition, it also warrants a clinical study to investigate the impact of *CYP2C8*3* and *CYP2C8*4* on imatinib pharmacokinetics (including N-desmethyl imatinib concentrations) and clinical response. Findings from these studies will provide valuable information for the individualised dosing of imatinib that might help in minimising the primary resistance and adverse events associated with imatinib treatment.

References

Aquilante, C. L., M. Niemi, L. Gong, R. B. Altman and T. E. Klein (2013a). PharmGKB summary: very important pharmacogene information for cytochrome P450, family 2, subfamily C, polypeptide 8. Pharmacogenet Genomics **23**(12): 721-728.

Aquilante, C. L., M. F. Wempe, S. H. Spencer, L. A. Kosmiski, J. A. Predhomme and M. S. Sidhom (2013b). Influence of CYP2C8*2 on the pharmacokinetics of pioglitazone in healthy African-American volunteers. Pharmacotherapy **33**(9): 1000-1007.

Baccarani, M., J. Cortes, F. Pane, D. Niederwieser, G. Saglio, J. Apperley, F. Cervantes, M. Deininger, A. Gratwohl, F. Guilhot, A. Hochhaus, M. Horowitz, T. Hughes, H. Kantarjian, R. Larson, J. Radich, B. Simonsson, R. T. Silver, J. Goldman and R. Hehlmann (2009). Chronic myeloid leukemia: an update of concepts and management recommendations of European LeukemiaNet. J Clin Oncol **27**(35): 6041-6051.

Bahadur, N., J. B. Leathart, E. Mutch, D. Steimel-Crespi, S. A. Dunn, R. Gilissen, J. V. Houdt, J. Hendrickx, G. Mannens, H. Bohets, F. M. Williams, M. Armstrong, C. L. Crespi and A. K. Daly (2002). CYP2C8 polymorphisms in Caucasians and their relationship with paclitaxel 6alpha-hydroxylase activity in human liver microsomes. Biochem Pharmacol **64**(11): 1579-1589.

Bajpai, P., S. Srinivasan, J. Ghosh, L. D. Nagy, S. Wei, F. P. Guengerich and N. G. Avadhani (2014). Targeting of splice variants of human cytochrome P450 2C8 (CYP2C8) to mitochondria and their role in arachidonic acid metabolism and respiratory dysfunction. J Biol Chem **289**(43): 29614-29630.

Baldwin, S. J., S. E. Clarke and R. J. Chenery (1999). Characterization of the cytochrome P450 enzymes involved in the in vitro metabolism of rosiglitazone. Br J Clin Pharmacol **48**(3): 424-432.

Berglund, E., S. J. Ubhayasekera, F. Karlsson, P. Akcakaya, W. Aluthgedara, J. Ahlen, R. Frobom, I. L. Nilsson, W. O. Lui, C. Larsson, J. Zedenius, J. Bergquist and R. Branstrom (2014). Intracellular concentration of the tyrosine kinase inhibitor imatinib in gastrointestinal stromal tumor cells. Anticancer Drugs **25**(4): 415-422.

Bergmann, T. K., C. Brasch-Andersen, H. Green, M. Mirza, R. S. Pedersen, F. Nielsen, K. Skougaard, J. Wihl, N. Keldsen, P. Damkier, L. E. Friberg, C. Peterson, W. Vach, M. O. Karlsson and K. Brosen (2011). Impact of CYP2C8*3 on paclitaxel clearance: a population pharmacokinetic and pharmacogenomic study in 93 patients with ovarian cancer. Pharmacogenomics J **11**(2): 113-120.

Bidstrup, T. B., I. Bjornsdottir, U. G. Sidelmann, M. S. Thomsen and K. T. Hansen (2003). CYP2C8 and CYP3A4 are the principal enzymes involved in the human in vitro biotransformation of the insulin secretagogue repaglinide. Br J Clin Pharmacol **56**(3): 305-314.

Bidstrup, T. B., P. Damkier, A. K. Olsen, M. Ekblom, A. Karlsson and K. Brosen (2006). The impact of CYP2C8 polymorphism and grapefruit juice on the pharmacokinetics of repaglinide. Br J Clin Pharmacol **61**(1): 49-57.

Bolton, A. E., B. Peng, M. Hubert, A. Krebs-Brown, R. Capdeville, U. Keller and M. Seiberling (2004). Effect of rifampicin on the pharmacokinetics of imatinib mesylate (Gleevec, STI571) in healthy subjects. Cancer Chemother Pharmacol **53**(2): 102-106.

Bouchet, S., K. Titier, N. Moore, R. Lassalle, B. Ambrosino, S. Poulette, P. Schuld, C. Belanger, F. X. Mahon and M. Molimard (2013). Therapeutic drug monitoring of imatinib in chronic myeloid leukemia: experience from 1216 patients at a centralized laboratory. Fundam Clin Pharmacol **27**(6): 690-697.

Bun, S. S., J. Ciccolini, H. Bun, C. Aubert and J. Catalin (2003). Drug interactions of paclitaxel metabolism in human liver microsomes. J Chemother **15**(3): 266-274.

Cytochrome P450 (CYP) allele nomenclature database URL: http://cypalleles.ki.se (accessed: Jan 2015).

Dai, D., D. C. Zeldin, J. A. Blaisdell, B. Chanas, S. J. Coulter, B. I. Ghanayem and J. A. Goldstein (2001). Polymorphisms in human CYP2C8 decrease metabolism of the anticancer drug paclitaxel and arachidonic acid. Pharmacogenetics **11**(7): 597-607.

Daily, E. B. and C. L. Aquilante (2009). Cytochrome P450 2C8 pharmacogenetics: a review of clinical studies. Pharmacogenomics **10**(9): 1489-1510.

Daley, G., R. Van Etten and D. Baltimore (1990). Induction of chronic myelogenous leukemia in mice by the P210bcr/abl gene of the Philadelphia chromosome. Science **247**(4944): 824-830.

de Wit, D., H. J. Guchelaar, J. den Hartigh, H. Gelderblom and N. P. van Erp (2015). Individualized dosing of tyrosine kinase inhibitors: are we there yet? Drug Discov Today **20**(1): 18-36.

Deininger, M., S. G. O'Brien, F. Guilhot, J. M. Goldman, A. Hochhaus, T. P. Hughes, J. P. Radich, A. K. Hatfield, M. Mone, J. Filian, J. Reynolds, I. Gathmann, R. A. Larson and B. J. Druker (2009). International randomized study of interferon vs STI571 (IRIS) 8-year follow up:

Sustained survival and low risk for progression or events in patients with newly diagnosed chronic myeloid leukemia in chronic phase (CML-CP) treated with imatinib. ASH annual meeting abstracts Blood **114**: 1126.

Delozier, T. C., G. E. Kissling, S. J. Coulter, D. Dai, J. F. Foley, J. A. Bradbury, E. Murphy, C. Steenbergen, D. C. Zeldin and J. A. Goldstein (2007). Detection of human CYP2C8, CYP2C9, and CYP2J2 in cardiovascular tissues. Drug Metab Dispos **35**(4): 682-688.

Di Gion, P., F. Kanefendt, A. Lindauer, M. Scheffler, O. Doroshyenko, U. Fuhr, J. Wolf and U. Jaehde (2011). Clinical pharmacokinetics of tyrosine kinase inhibitors: focus on pyrimidines, pyridines and pyrroles. Clin Pharmacokinet **50**(9): 551-603.

Druker, B. J., F. Guilhot, S. G. O'Brien, I. Gathmann, H. Kantarjian, N. Gattermann, M. W. N. Deininger, R. T. Silver, J. M. Goldman, R. M. Stone, F. Cervantes, A. Hochhaus, B. L. Powell, J. L. Gabrilove, P. Rousselot, J. Reiffers, J. J. Cornelissen, T. Hughes, H. Agis, T. Fischer, G. Verhoef, J. Shepherd, G. Saglio, A. Gratwohl, J. L. Nielsen, J. P. Radich, B. Simonsson, K. Taylor, M. Baccarani, C. So, L. Letvak and R. A. Larson (2006). Five-year follow-up of patients receiving imatinib for chronic myeloid leukemia. N Engl J Med **355**(23): 2408-2417.

Druker, B. J., M. Talpaz, D. J. Resta, B. Peng, E. Buchdunger, J. M. Ford, N. B. Lydon, H. Kantarjian, R. Capdeville, S. Ohno-Jones and C. L. Sawyers (2001). Efficacy and safety of a specific inhibitor of the BCR-ABL tyrosine kinase in chronic myeloid leukemia. N Engl J Med **344**(14): 1031-1037.

Dutreix, C., B. Peng, G. Mehring, M. Hayes, R. Capdeville, R. Pokorny and M. Seiberling (2004). Pharmacokinetic interaction between ketoconazole and imatinib mesylate (Glivec) in healthy subjects. Cancer Chemother Pharmacol **54**(4): 290-294.

Fasinu, P., P. J. Bouic and B. Rosenkranz (2012). Liver-based in vitro technologies for drug biotransformation studies - a review. Curr Drug Metab **13**(2): 215-224.

FDA (2011). Drug development and drug interactions. Table of substrates, inhibitors and inducers. URL:http://www.fda.gov/Drugs/DevelopmentApprovalProcess/DevelopmentResources/DrugInteractionsLabeling/ucm093664.htm, acessed Jan, 2015.

Filppula, A.M (2014), PhD dessertation. Role of CYP2C8 in the metabolism of montelukast and imatinib, studies in vitro, in silico and in humans. Available online: https://helda.helsinki.fi/bitstream/handle/10138/136331/roleofcy.pdf?sequence=1, acessed Jan, 2015.

Filppula, A. M., J. Laitila, P. J. Neuvonen and J. T. Backman (2012). Potent mechanism-based inhibition of CYP3A4 by imatinib explains its liability to interact with CYP3A4 substrates. Br J Pharmacol **165**(8): 2787-2798.

Filppula, A. M., M. Neuvonen, J. Laitila, P. J. Neuvonen and J. T. Backman (2013a). Autoinhibition of CYP3A4 leads to important role of CYP2C8 in imatinib metabolism: variability in CYP2C8 activity may alter plasma concentrations and response. Drug Metab Dispos **41**(1): 50-59.

Filppula, A. M., A. Tornio, M. Niemi, P. J. Neuvonen and J. T. Backman (2013b). Gemfibrozil impairs imatinib absorption and inhibits the CYP2C8-mediated formation of its main metabolite. Clin Pharmacol Ther **94**(3): 383-393.

Gao, Y., D. Liu, H. Wang, J. Zhu and C. Chen (2010). Functional characterization of five CYP2C8 variants and prediction of CYP2C8 genotype-dependent effects on in vitro and in vivo drug-drug interactions. Xenobiotica **40**(7): 467-475.

Garfinkel, D. (1958). Studies on pig liver microsomes. I. Enzymic and pigment composition of different microsomal fractions. Arch Biochem Biophys **77**(2): 493-509.

Goldman, J. M. and J. V. Melo (2003). Chronic myeloid leukemia--advances in biology and new approaches to treatment. N Engl J Med **349**(15): 1451-1464.

Gotta, V., S. Bouchet, N. Widmer, P. Schuld, L. A. Decosterd, T. Buclin, F. X. Mahon, C. Csajka and M. Molimard (2014). Large-scale imatinib dose-concentration-effect study in CML patients under routine care conditions. Leuk Res **38**(7): 764-772.

Green, H., P. Soderkvist, P. Rosenberg, R. A. Mirghani, P. Rymark, E. A. Lundqvist and C. Peterson (2009). Pharmacogenetic studies of Paclitaxel in the treatment of ovarian cancer. Basic Clin Pharmacol Toxicol **104**(2): 130-137.

Gschwind, H. P., U. Pfaar, F. Waldmeier, M. Zollinger, C. Sayer, P. Zbinden, M. Hayes, R. Pokorny, M. Seiberling, M. Ben-Am, B. Peng and G. Gross (2005). Metabolism and disposition of imatinib mesylate in healthy volunteers. Drug Metab Dispos **33**(10): 1503-1512.

Guengerich, F. P. (2008). Cytochrome p450 and chemical toxicology. Chem Res Toxicol **21**(1): 70-83.

Guilhot, F., T. P. Hughes, J. Cortes, B. J. Druker, M. Baccarani, I. Gathmann, M. Hayes, C. Granvil and Y. Wang (2012). Plasma exposure of imatinib and its correlation with clinical response in the Tyrosine Kinase Inhibitor Optimization and Selectivity Trial. Haematologica **97**(5): 731-738.

Hamman, M. A., G. A. Thompson and S. D. Hall (1997). Regioselective and stereoselective metabolism of ibuprofen by human cytochrome P450 2C. Biochem Pharmacol **54**(1): 33-41.

Hanfstein, B., M. C. Muller, R. Hehlmann, P. Erben, M. Lauseker, A. Fabarius, S. Schnittger, C. Haferlach, G. Gohring, U. Proetel, H. J. Kolb, S. W. Krause, W. K. Hofmann, J. Schubert, H. Einsele, J. Dengler, M. Hanel, C. Falge, L. Kanz, A. Neubauer, M. Kneba, F. Stegelmann, M. Pfreundschuh, C. F. Waller, S. Branford, T. P. Hughes, K. Spiekermann, G. M. Baerlocher, M. Pfirrmann, J. Hasford, S. Saussele and A. Hochhaus (2012). Early molecular and cytogenetic response is predictive for long-term progression-free and overall survival in chronic myeloid leukemia (CML). Leukemia **26**(9): 2096-2102.

Hendrychova, T., E. Anzenbacherova, J. Hudecek, J. Skopalik, R. Lange, P. Hildebrandt, M. Otyepka and P. Anzenbacher (2011). Flexibility of human cytochrome P450 enzymes: molecular dynamics and spectroscopy reveal important function-related variations. Biochim Biophys Acta **1814**(1): 58-68.

Hichiya, H., T. Tanaka-Kagawa, A. Soyama, H. Jinno, S. Koyano, N. Katori, E. Matsushima, S. Uchiyama, H. Tokunaga, H. Kimura, N. Minami, M. Katoh, K. Sugai, Y. Goto, T. Tamura, N. Yamamoto, Y. Ohe, H. Kunitoh, H. Nokihara, T. Yoshida, H. Minami, N. Saijo, M. Ando, S. Ozawa, Y. Saito and J. Sawada (2005). Functional characterization of five novel CYP2C8 variants, G171S, R186X, R186G, K247R, and K383N, found in a Japanese population. Drug Metab Dispos **33**(5): 630-636.

Houston, J. B. and A. Galetin (2005). Modelling atypical CYP3A4 kinetics: principles and pragmatism. Arch Biochem Biophys **433**(2): 351-360.

Houston, J. B. and K. E. Kenworthy (2000). In vitro-in vivo scaling of CYP kinetic data not consistent with the classical Michaelis-Menten model. Drug Metab Dispos **28**(3): 246-254.

Jaakkola, T., J. Laitila, P. J. Neuvonen and J. T. Backman (2006). Pioglitazone is metabolised by CYP2C8 and CYP3A4 in vitro: potential for interactions with CYP2C8 inhibitors. Basic Clin Pharmacol Toxicol **99**(1): 44-51.

Jabbour, E. and H. Kantarjian (2014). Chronic myeloid leukemia: 2014 update on diagnosis, monitoring, and management. Am J Hematol **89**(5): 547-556.

Jabbour, E. J., J. E. Cortes and H. M. Kantarjian (2013). Resistance to tyrosine kinase inhibition therapy for chronic myelogenous leukemia: a clinical perspective and emerging treatment options. Clin Lymphoma Myeloma Leuk **13**(5): 515-529.

Jiang, H., F. Zhong, L. Sun, W. Feng, Z. X. Huang and X. Tan (2011). Structural and functional insights into polymorphic enzymes of cytochrome P450 2C8. Amino Acids **40**(4): 1195-1204.

Josephs, D. H., D. S. Fisher, J. Spicer and R. J. Flanagan (2013). Clinical pharmacokinetics of tyrosine kinase inhibitors: implications for therapeutic drug monitoring. Ther Drug Monit **35**(5): 562-587.

Kalmanti, L., S. Saussele, M. Lauseker, M. C. Muller, C. T. Dietz, L. Heinrich, B. Hanfstein, U. Proetel, A. Fabarius, S. W. Krause, S. Rinaldetti, J. Dengler, C. Falge, E. Oppliger-Leibundgut, A. Burchert, A. Neubauer, L. Kanz, F. Stegelmann, M. Pfreundschuh, K. Spiekermann, C. Scheid, M. Pfirrmann, A. Hochhaus, J. Hasford and R. Hehlmann (2015). Safety and efficacy of imatinib in cml over a period of 10 years: data from the randomized cml-study iv. Leukemia.

Kim, K. A., J. Chung, D. H. Jung and J. Y. Park (2004). Identification of cytochrome P450 isoforms involved in the metabolism of loperamide in human liver microsomes. Eur J Clin Pharmacol **60**(8): 575-581.

Kim, K. A., J. Y. Park, J. S. Lee and S. Lim (2003). Cytochrome P450 2C8 and CYP3A4/5 are involved in chloroquine metabolism in human liver microsomes. Arch Pharm Res **26**(8): 631-637.

Kirchheiner, J., S. Thomas, S. Bauer, D. Tomalik-Scharte, U. Hering, O. Doroshyenko, A. Jetter, S. Stehle, M. Tsahuridu, I. Meineke, J. Brockmoller and U. Fuhr (2006). Pharmacokinetics and pharmacodynamics of rosiglitazone in relation to CYP2C8 genotype. Clin Pharmacol Ther **80**(6): 657-667.

Klees, T. M., P. Sheffels, O. Dale and E. D. Kharasch (2005). Metabolism of alfentanil by cytochrome p4503a (cyp3a) enzymes. Drug Metab Dispos **33**(3): 303-311.

Klingenberg, M. (1958). Pigments of rat liver microsomes. Arch Biochem Biophys **75**(2): 376-386.

Klose, T. S., J. A. Blaisdell and J. A. Goldstein (1999). Gene structure of CYP2C8 and extrahepatic distribution of the human CYP2Cs. J Biochem Mol Toxicol **13**(6): 289-295.

Kretz, O., H. M. Weiss, M. M. Schumacher and G. Gross (2004). In vitro blood distribution and plasma protein binding of the tyrosine kinase inhibitor imatinib and its active metabolite, CGP74588, in rat, mouse, dog, monkey, healthy humans and patients with acute lymphatic leukaemia. Br J Clin Pharmacol **58**(2): 212-216.

Lai, X. S., L. P. Yang, X. T. Li, J. P. Liu, Z. W. Zhou and S. F. Zhou (2009). Human CYP2C8: structure, substrate specificity, inhibitor selectivity, inducers and polymorphisms. Curr Drug Metab **10**(9): 1009-1047.

Lankheet, N. A., L. M. Knapen, J. H. Schellens, J. H. Beijnen, N. Steeghs and A. D. Huitema (2014). Plasma concentrations of tyrosine kinase inhibitors imatinib, erlotinib, and sunitinib in routine clinical outpatient cancer care. Ther Drug Monit **36**(3): 326-334.

Larson, R. A., B. J. Druker, F. Guilhot, S. G. O'Brien, G. J. Riviere, T. Krahnke, I. Gathmann and Y. Wang (2008). Imatinib pharmacokinetics and its correlation with response and safety in chronic-phase chronic myeloid leukemia: a subanalysis of the IRIS study. Blood **111**(8): 4022-4028.

Lawrence, S. K., D. Nguyen, C. Bowen, L. Richards-Peterson and K. W. Skordos (2014). The metabolic drug-drug interaction profile of Dabrafenib: in vitro investigations and quantitative extrapolation of the P450-mediated DDI risk. Drug Metab Dispos **42**(7): 1180-1190.

Leukaemia foundation Australia URL: http://leukaemia.org.au/blood-cancers/leukaemias/chronic-lymphocytic-leukaemia-cll, accessed: Jan 2015.

Li, X. Q., A. Bjorkman, T. B. Andersson, M. Ridderstrom and C. M. Masimirembwa (2002). Amodiaquine clearance and its metabolism to N-desethylamodiaquine is mediated by CYP2C8: a new high affinity and turnover enzyme-specific probe substrate. J Pharmacol Exp Ther **300**(2): 399-407.

Li, Y., J. K. Coller, M. R. Hutchinson, K. Klein, U. M. Zanger, N. J. Stanley, A. D. Abell and A. A. Somogyi (2013). The CYP2B6*6 allele significantly alters the N-demethylation of ketamine enantiomers in vitro. Drug Metab Dispos **41**(6): 1264-1272.

Linch, M., J. Claus and C. Benson (2013). Update on imatinib for gastrointestinal stromal tumors: duration of treatment. Onco Targets Ther **6**: 1011-1023.

Maino, E., R. Sancetta, P. Viero, S. Imbergamo, A. M. Scattolin, M. Vespignani and R. Bassan (2014). Current and future management of Ph/BCR-ABL positive ALL. Expert Rev Anticancer Ther **14**(6): 723-740.

Marin, D., A. Bazeos, F. X. Mahon, L. Eliasson, D. Milojkovic, M. Bua, J. F. Apperley, R. Szydlo, R. Desai, K. Kozlowski, C. Paliompeis, V. Latham, L. Foroni, M. Molimard, A. Reid, K. Rezvani, H. de Lavallade, C. Guallar, J. Goldman and J. S. Khorashad (2010). Adherence is the critical factor for achieving molecular responses in patients with chronic myeloid leukemia who achieve complete cytogenetic responses on imatinib. J Clin Oncol **28**(14): 2381-2388.

Marin, D., A. R. Ibrahim, C. Lucas, G. Gerrard, L. Wang, R. M. Szydlo, R. E. Clark, J. F. Apperley, D. Milojkovic, M. Bua, J. Pavlu, C. Paliompeis, A. Reid, K. Rezvani, J. M. Goldman and L. Foroni (2012). Assessment of BCR-ABL1 transcript levels at 3 months is the only requirement for predicting outcome for patients with chronic myeloid leukemia treated with tyrosine kinase inhibitors. J Clin Oncol **30**(3): 232-238.

Marsh, S., G. Somlo, X. Li, P. Frankel, C. R. King, W. D. Shannon, H. L. McLeod and T. W. Synold (2007). Pharmacogenetic analysis of paclitaxel transport and metabolism genes in breast cancer. Pharmacogenomics J **7**(5): 362-365.

Marull, M. and B. Rochat (2006). Fragmentation study of imatinib and characterization of new imatinib metabolites by liquid chromatography-triple-quadrupole and linear ion trap mass spectrometers. J Mass Spectrom **41**(3): 390-404.

Michallet, M., M. Tulliez, S. Corm, M. Gardembas, F. Huguet, A. Oukessou, B. Bregman, A. Vekhoff, K. Ghomari, N. Cambier and A. Guerci-Bresler (2010). Management of chronic myeloid leukaemia in clinical practice in France: results of the French subset of patients from the UNIC study. Curr Med Res Opin **26**(2): 307-317.

Miners, J. O., P. I. Mackenzie and K. M. Knights (2010). The prediction of drug-glucuronidation parameters in humans: UDP-glucuronosyltransferase enzyme-selective substrate and inhibitor probes for reaction phenotyping and in vitro-in vivo extrapolation of drug clearance and drug-drug interaction potential. Drug Metab Rev **42**(1): 196-208.

Muschler, E., J. Lal, A. Jetter, A. Rattay, U. Zanger, G. Zadoyan, U. Fuhr and J. Kirchheiner (2009). The role of human CYP2C8 and CYP2C9 variants in pioglitazone metabolism in vitro. Basic Clin Pharmacol Toxicol **105**(6): 374-379.

Nebert, D. W. and D. W. Russell (2002). Clinical importance of the cytochromes P450. Lancet **360**(9340): 1155-1162.

Nebot, N., S. Crettol, F. d'Esposito, B. Tattam, D. E. Hibbs and M. Murray (2010). Participation of CYP2C8 and CYP3A4 in the N-demethylation of imatinib in human hepatic microsomes. Br J Pharmacol **161**(5): 1059-1069.

Neelakantan, P., G. Gerrard, C. Lucas, D. Milojkovic, P. May, L. Wang, C. Paliompeis, M. Bua, A. Reid, K. Rezvani, S. O'Brien, R. Clark, J. Goldman and D. Marin (2013). Combining BCR-ABL1 transcript levels at 3 and 6 months in chronic myeloid leukemia: implications for early intervention strategies. Blood **121**(14): 2739-2742.

Nelson, D. R. (2006). Cytochrome P450 nomenclature, 2004. Methods Mol Biol **320**: 1-10.

Niemi, M., J. B. Leathart, M. Neuvonen, J. T. Backman, A. K. Daly and P. J. Neuvonen (2003). Polymorphism in CYP2C8 is associated with reduced plasma concentrations of repaglinide. Clin Pharmacol Ther **74**(4): 380-387.

Ogilvie, B. W., D. Zhang, W. Li, A. D. Rodrigues, A. E. Gipson, J. Holsapple, P. Toren and A. Parkinson (2006). Glucuronidation converts gemfibrozil to a potent, metabolism-dependent inhibitor of CYP2C8: implications for drug-drug interactions. Drug Metab Dispos **34**(1): 191-197.

Ohyama, K., M. Nakajima, S. Nakamura, N. Shimada, H. Yamazaki and T. Yokoi (2000). A significant role of human cytochrome P450 2C8 in amiodarone N-deethylation: an approach to predict the contribution with relative activity factor. Drug Metab Dispos **28**(11): 1303-1310.

Ong, C. E., Y. Pan, J. W. Mak and R. Ismail (2013). In vitro approaches to investigate cytochrome P450 activities: update on current status and their applicability. Expert Opin Drug Metab Toxicol **9**(9): 1097-1113.

Parikh, S., J. B. Ouedraogo, J. A. Goldstein, P. J. Rosenthal and D. L. Kroetz (2007). Amodiaquine metabolism is impaired by common polymorphisms in CYP2C8: implications for malaria treatment in Africa. Clin Pharmacol Ther **82**(2): 197-203.

Pelkonen, O. and M. Turpeinen (2007). In vitro-in vivo extrapolation of hepatic clearance: biological tools, scaling factors, model assumptions and correct concentrations. Xenobiotica **37**(10-11): 1066-1089.

Pelkonen, O., M. Turpeinen, J. Hakkola, P. Honkakoski, J. Hukkanen and H. Raunio (2008). Inhibition and induction of human cytochrome P450 enzymes: current status. Arch Toxicol **82**(10): 667-715.

Peng, B., C. Dutreix, G. Mehring, M. J. Hayes, M. Ben-Am, M. Seiberling, R. Pokorny, R. Capdeville and P. Lloyd (2004). Absolute bioavailability of imatinib (Glivec) orally versus intravenous infusion. J Clin Pharmacol **44**(2): 158-162.

Peng, B., P. Lloyd and H. Schran (2005). Clinical pharmacokinetics of imatinib. Clin Pharmacokinet **44**(9): 879-894.

Picard, N., T. Cresteil, N. Djebli and P. Marquet (2005). In vitro metabolism study of buprenorphine: evidence for new metabolic pathways. Drug Metab Dispos **33**(5): 689-695.

Picard, S., K. Titier, G. Etienne, E. Teilhet, D. Ducint, M. A. Bernard, R. Lassalle, G. Marit, J. Reiffers, B. Begaud, N. Moore, M. Molimard and F. X. Mahon (2007). Trough imatinib plasma levels are associated with both cytogenetic and molecular responses to standard-dose imatinib in chronic myeloid leukemia. Blood **109**(8): 3496-3499.

Rahman, A., K. R. Korzekwa, J. Grogan, F. J. Gonzalez and J. W. Harris (1994). Selective biotransformation of taxol to 6 alpha-hydroxytaxol by human cytochrome P450 2C8. Cancer Res **54**(21): 5543-5546.

Rang, H.P, Dale, M.M and Ritter, J.M (1999). Drug elimination and pharmacokinetics. In : Pharmacology 4th Edition. p 80-92. Churchill Livingstone.

Rebbeck, T. R., J. M. Jaffe, A. H. Walker, A. J. Wein and S. B. Malkowicz (1998). Modification of clinical presentation of prostate tumors by a novel genetic variant in CYP3A4. J Natl Cancer Inst **90**(16): 1225-1229.

Rochat, B., V. Zoete, A. Grosdidier, S. von Grunigen, M. Marull and O. Michielin (2008). In vitro biotransformation of imatinib by the tumor expressed CYP1A1 and CYP1B1. Biopharm Drug Dispos **29**(2): 103-118.

Rowbotham, S. E., A. V. Boddy, C. P. Redfern, G. J. Veal and A. K. Daly (2010). Relevance of nonsynonymous CYP2C8 polymorphisms to 13-cis retinoic acid and paclitaxel hydroxylation. Drug Metab Dispos **38**(8): 1261-1266.

Schmidli, H., B. Peng, G. J. Riviere, R. Capdeville, M. Hensley, I. Gathmann, A. E. Bolton and A. Racine-Poon (2005). Population pharmacokinetics of imatinib mesylate in patients with chronic-phase chronic myeloid leukaemia: results of a phase III study. Br J Clin Pharmacol **60**(1): 35-44.

Schoch, G. A., J. K. Yano, S. Sansen, P. M. Dansette, C. D. Stout and E. F. Johnson (2008). Determinants of cytochrome P450 2C8 substrate binding: structures of complexes with montelukast, troglitazone, felodipine, and 9-cis-retinoic acid. J Biol Chem **283**(25): 17227-17237.

Silverman, R.B (1995). Mechanism-based enzyme inactivators. Methods Enzymol 249: 240-283

Singh, R., J. G. Ting, Y. Pan, L. K. Teh, R. Ismail and C. E. Ong (2008). Functional role of Ile264 in CYP2C8: mutations affect haem incorporation and catalytic activity. Drug Metab Pharmacokinet **23**(3): 165-174.

Sohn, S. K., S. J. Oh, B. S. Kim, H. M. Ryoo, J. S. Chung, Y. D. Joo, S. M. Bang, C. W. Jung, D. H. Kim, S. S. Yoon, H. Kim, H. G. Lee, J. H. Won, Y. H. Min, J. W. Cheong, J. S. Park, K. S. Eom, M. S. Hyun, M. K. Kim, H. Kim, M. R. Park, J. Park, C. S. Kim, H. J. Kim, Y. K. Kim, E. K. Park, D. Y. Zang, D. Y. Jo, J. H. Moon and S. Y. Park (2011). Trough plasma imatinib levels are correlated with optimal cytogenetic responses at 6 months after treatment with standard dose of imatinib in newly diagnosed chronic myeloid leukemia. Leuk Lymphoma **52**(6): 1024-1029.

Soyama, A., Y. Saito, N. Hanioka, N. Murayama, O. Nakajima, N. Katori, S. Ishida, K. Sai, S. Ozawa and J. I. Sawada (2001). Non-synonymous single nucleotide alterations found in the CYP2C8 gene result in reduced in vitro paclitaxel metabolism. Biol Pharm Bull **24**(12): 1427-1430.

Stage, T. B., M. M. Christensen, S. Feddersen, H. Beck-Nielsen and K. Brosen (2013). The role of genetic variants in CYP2C8, LPIN1, PPARGC1A and PPARgamma on the trough steady-state plasma concentrations of rosiglitazone and on glycosylated haemoglobin A1c in type 2 diabetes. Pharmacogenet Genomics **23**(4): 219-227.

Takahashi, N., H. Wakita, M. Miura, S. A. Scott, K. Nishii, M. Masuko, M. Sakai, Y. Maeda, K. Ishige, M. Kashimura, K. Fujikawa, M. Fukazawa, T. Katayama, F. Monma, M. Narita, F. Urase, T. Furukawa, Y. Miyazaki, N. Katayama and K. Sawada (2010). Correlation between imatinib pharmacokinetics and clinical response in japanese patients with chronic-phase chronic myeloid leukemia. Clin Pharmacol Ther **88**(6): 809-813.

Tan, K. L., R. Ankathil and S. H. Gan (2011). Method development and validation for the simultaneous determination of imatinib mesylate and N-desmethyl imatinib using rapid resolution high performance liquid chromatography coupled with UV-detection. J Chromatogr B Analyt Technol Biomed Life Sci **879**(30): 3583-3591.

Taniguchi, R., T. Kumai, N. Matsumoto, M. Watanabe, K. Kamio, S. Suzuki and S. Kobayashi (2005). Utilization of human liver microsomes to explain individual differences in paclitaxel metabolism by CYP2C8 and CYP3A4. J Pharmacol Sci **97**(1): 83-90.

Tomalik-Scharte, D., U. Fuhr, M. Hellmich, D. Frank, O. Doroshyenko, A. Jetter and J. C. Stingl (2011). Effect of the CYP2C8 genotype on the pharmacokinetics and pharmacodynamics of repaglinide. Drug Metab Dispos **39**(5): 927-932.

Tornio, A., A. M. Filppula, O. Kailari, M. Neuvonen, T. H. Nyronen, T. Tapaninen, P. J. Neuvonen, M. Niemi and J. T. Backman (2014). Glucuronidation converts clopidogrel to a strong time-dependent inhibitor of CYP2C8: a phase II metabolite as a perpetrator of drug-drug interactions. Clin Pharmacol Ther **96**(4): 498-507.

Tornio, A., M. Niemi, P. J. Neuvonen and J. T. Backman (2008). Trimethoprim and the CYP2C8*3 allele have opposite effects on the pharmacokinetics of pioglitazone. Drug Metab Dispos **36**(1): 73-80.

Totah, R. A. and A. E. Rettie (2005). Cytochrome P450 2C8: substrates, inhibitors, pharmacogenetics, and clinical relevance. Clin Pharmacol Ther **77**(5): 341-352.

van Erp, N. P., H. Gelderblom, M. O. Karlsson, J. Li, M. Zhao, J. Ouwerkerk, J. W. Nortier, H. J. Guchelaar, S. D. Baker and A. Sparreboom (2007). Influence of CYP3A4 inhibition on the steady-state pharmacokinetics of imatinib. Clin Cancer Res **13**(24): 7394-7400.

Walsky, R. L., R. S. Obach, E. A. Gaman, J. P. Gleeson and W. R. Proctor (2005). Selective inhibition of human cytochrome P4502C8 by montelukast. Drug Metab Dispos **33**(3): 413-418.

Wang, D., Y. Guo, S. A. Wrighton, G. E. Cooke and W. Sadee (2011). Intronic polymorphism in CYP3A4 affects hepatic expression and response to statin drugs. Pharmacogenomics J **11**(4): 274-286.

Wang, J. S., M. Neuvonen, X. Wen, J. T. Backman and P. J. Neuvonen (2002). Gemfibrozil inhibits CYP2C8-mediated cerivastatin metabolism in human liver microsomes. Drug Metab Dispos **30**(12): 1352-1356.

Wang, Y., M. Wang, H. Qi, P. Pan, T. Hou, J. Li, G. He and H. Zhang (2014a). Pathway-dependent inhibition of paclitaxel hydroxylation by kinase inhibitors and assessment of drug-drug interaction potentials. Drug Metab Dispos **42**(4): 782-795.

Wang, Z., S. Wang, M. Huang, H. Hu, L. Yu and S. Zeng (2014b). Characterizing the effect of cytochrome P450 (CYP) 2C8, CYP2C9, and CYP2D6 genetic polymorphisms on stereoselective N-demethylation of fluoxetine. Chirality **26**(3): 166-173.

Wattanachai, N., T. M. Polasek, T. M. Heath, V. Uchaipichat, W. Tassaneeyakul, W. Tassaneeyakul and J. O. Miners (2011). In vitro-in vivo extrapolation of CYP2C8-catalyzed paclitaxel 6alpha-hydroxylation: effects of albumin on in vitro kinetic parameters and assessment of interindividual variability in predicted clearance. Eur J Clin Pharmacol **67**(8): 815-824.

Wen, X., J. S. Wang, J. T. Backman, K. T. Kivisto and P. J. Neuvonen (2001). Gemfibrozil is a potent inhibitor of human cytochrome P450 2C9. Drug Metab Dispos **29**(11): 1359-1361.

Widmer, N., L. A. Decosterd, C. Csajka, S. Leyvraz, M. A. Duchosal, A. Rosselet, B. Rochat, C. B. Eap, H. Henry, J. Biollaz and T. Buclin (2006). Population pharmacokinetics of imatinib and the role of alpha-acid glycoprotein. Br J Clin Pharmacol **62**(1): 97-112.

Widmer, N., C. Bardin, E. Chatelut, A. Paci, J. Beijnen, D. Leveque, G. Veal and A. Astier (2014). Review of therapeutic drug monitoring of anticancer drugs part two--targeted therapies. Eur J Cancer **50**(12): 2020-2036.

Wilkinson, G. R. (2005). Drug metabolism and variability among patients in drug response. N Engl J Med **352**(21): 2211-2221.

Yasar, U., S. Lundgren, E. Eliasson, A. Bennet, B. Wiman, U. de Faire and A. Rane (2002). Linkage between the CYP2C8 and CYP2C9 genetic polymorphisms. Biochem Biophys Res Commun **299**(1): 25-28.

Yeung, D. T. and D. L. White (2011). Imatinib trough levels in chronic myelogenous leukemia: does one dose fit all? Leuk Lymphoma **52**(2): 165-167.

Yu, L., D. Shi, L. Ma, Q. Zhou and S. Zeng (2013). Influence of CYP2C8 polymorphisms on the hydroxylation metabolism of paclitaxel, repaglinide and ibuprofen enantiomers in vitro. Biopharm Drug Dispos **34**(5): 278-287.

Zanger, U. M. and M. Schwab (2013). Cytochrome P450 enzymes in drug metabolism: regulation of gene expression, enzyme activities, and impact of genetic variation. Pharmacol Ther **138**(1): 103-141.

Zanger, U. M., F. Vilbois, J. P. Hardwick and U. A. Meyer (1988). Absence of hepatic cytochrome P450bufI causes genetically deficient debrisoquine oxidation in man. Biochemistry **27**(15): 5447-5454.

Khan, M.S., Barratt, D.T. & Somogyi, A.A. (2016). Impact of CYP2C8*3 polymorphism on in vitro metabolism of imatinib to N-desmethyl imatinib, *Xenobiotica, 46*(3), 278-287.